OPTIMAL OPERATION AND PLANNING OF ELECTRIC VEHICLES BATTERY SWAPPING STATIONS

by

Ahmed Ayman Ahmed Shalaby

A Thesis Presented to the Faculty of the
American University of Sharjah
College of Engineering
In Partial Fulfillment
of the Requirements
for the Degree of

Master of Science in
Electrical Engineering

Sharjah, United Arab Emirates

May 2020

Declaration of Authorship

I declare that this thesis is my own work and, to the best of my knowledge and belief, it does not contain material published or written by a third party, except where permission has been obtained and/or appropriately cited through full and accurate referencing.

Signed……………………Ahmed Ayman Ahmed Shalaby………………………….

Date…………………………………21/04/2021……………………………………

Approval Signatures

We, the undersigned, approve the Master's Thesis of Ahmed Ayman Ahmed Shalaby

Thesis Title: Optimal Planning and Operation of Electric Vehicles Battery Swapping Stations

Date of Defense: 19/04/2021

Name, Title and Affiliation	Signature
Dr. Mostafa Farouk Shaaban Associate Professor, Department of Electrical Engineering Thesis Advisor	
Dr. Mahmoud H. Ismail Professor, Department of Electrical Engineering Thesis Committee Member	
Dr. Hatem Zeineldin Professor, Department of Electrical and Computer Science, Khalifa University Thesis Committee Member	
Dr. Nasser Qaddoumi Head Department of Electrical Engineering	
Dr. Lotfi Romdhane Associate Dean for Graduate Affairs and Research College of Engineering	
Dr. Sameer Al-Asheh Interim Dean College of Engineering	
Dr. Mohamed El-Tarhuni Vice Provost for Graduate Studies Office of Graduate Studies	

Acknowledgment

Praise be to Allah, the Cherisher and Sustainer of the worlds, whose countless bounties enabled me to accomplish this thesis successfully

I would like to thank my supervisor Dr. Mostafa Farouk Shaaban for providing knowledge, guidance, support, and motivation throughout my research stages. I'm deeply beholden for his great assistance, worthy discussion, and suggestions.

I would like to thank the professors of the Electrical Engineering department who taught me the master level courses with mighty teaching methods and skills. I appreciate their dignified advice and motivation. I would also like to thank the American University of Sharjah for providing me with graduate assistantship which helped me to complete my thesis.

Lastly, I would like to thank my parents for their understanding, continuous support, and encouragement.

Abstract

Electric Vehicles (EVs) nowadays have become increasingly prevalent due to the advancements in EV technology and their impact on reducing greenhouse emissions. However, there are still some factors affecting the fast deployment of EVs such as the limited driving range and the charging time. Due to the limited driving range, EVs need to be charged frequently, but charging requires a long period at traditional EV charging stations, whereas fast-charging stations still have concerns regarding the wait and the charging time, which might cause traffic jams near the station. In this thesis, new dynamic optimal operation and planning approaches of EV battery-swapping stations (BSS) are introduced. In the operation phase, the goal is to maximize the daily profit using a rolling horizon optimization (RHO) mechanism and determining the optimal operating schedule for swapping and charging/discharging processes. The problem is formulated as mixed-integer linear programming (MILP) problem with nonlinear battery degradation characteristics included. Long-short-term memory (LSTM) recurrent neural network is used as a time series forecasting engine for predicting the EVs' arrivals. The proposed approach is tested and compared with the unscheduled operation and day-ahead scheduling. The results show that the dynamic operations scheduling using the proposed RHO mechanism results in a higher profit. In the second phase, an optimal planning approach for a photovoltaic-based BSS system is proposed considering the PV system and EV arrivals uncertainty. The main goal of the planning part is to determine the optimal size of the BSS assets and to optimally allocate the BSS in the distribution network. Markov Chain Monte Carlo Simulation is used to tackle the uncertainty associated with photovoltaic output and EV arrivals. Simulation results show the effectiveness of the proposed BSS system and an optimal solution is obtained which maximizes the annualized profit.

Keywords: ***Battery swapping stations; Battery-to-grid; EV charging stations; Electric Vehicles; Long short term memory; Optimization; Rolling Horizon, Markov Chain Monte Carlo Simulation.***

Table of Contents

Abstract.......5
List of Figures.......8
List of Tables.......9
List of Abbreviations.......10
Nomenclature.......12
Chapter 1 . Introduction.......17
1.1. Overview.......17
1.2. Thesis Objectives.......18
1.3. Research Contribution.......18
1.4. Thesis Organization.......18
Chapter 2 . Background and Literature Review.......20
2.1. Background on EVs Charging.......20
2.1.1. Fast charging stations.......20
2.1.2. Battery swapping stations.......21
2.2. Related Work.......21
2.2.1. BSS with renewable generation and microgrid.......22
2.2.2. BSSs serving a specific EV type.......23
2.2.3. Variable chargers and battery heterogeneity.......23
2.2.4. Demand forecasting.......23
2.2.5. Solving the optimization problem.......24
2.2.6. Rolling horizon predictive scheduling.......24
2.2.7. BSS planning.......25
Chapter 3 . Methodology.......26
3.1. The Structure of the Proposed BSS System.......26
3.1.1. Details of the system model.......26
3.1.2. Assumptions.......27

3.2. Optimization Model 27
3.2.1. The BSS mathematical model. 28
3.2.2. Battery heterogeneity. 31
3.2.3. Battery degradation effect. 31
3.2.3. Linearization. 32
Chapter 4 . Demand Forecasting 33
4.1. Rolling Horizon Predictive Controller 33
4.2. LSTM for Forecasting 34
Chapter 5 . Operation Case Studies and Simulation 37
5.1. Case Study I (Day-Ahead Scheduling for a Small Battery Stock) 38
5.2. Case Study II (Unscheduled Operation) 39
5.3. Case Study III (Day-Ahead Scheduling with Perfect Forecasting) 40
5.4. Case Study IV (Rolling Horizon Scheduling) 42
Chapter 6 . BSS Planning 45
6.1. System Costs 45
6.2. Modeling of PV 45
6.3. Modeling of EV Arrival Rates 50
6.4. Optimization Problem Formulation 51
6.4.1. The objective function. 51
6.4.2. Operation constraints of the PV-based BSS system. 53
6.4.3. Operation constraints of the distribution system. 54
6.5. Proposed Solution 55
6.6. Planning Results and Analysis 57
Chapter 7 . Conclusion 60
References 61
Vita 64

List of Figures

Figure 2.1: The BSS operations [7]. 21
Figure 3.1: The structure of the proposed BSS model. 26
Figure 4.1: Rolling horizon mechanism...33
Figure 4.2: The LSTM cell structure 36
Figure 5.1: Day-ahead scheduling for a small battery stock. 39
Figure 5.2. Unscheduled operation of BSS while charging as soon as possible 39
Figure 5.3: The profit and the number of EV arrivals in the unscheduled operation. .40
Figure 5.4. Day-ahead operation of the BSS 41
Figure 5.5: The profit and the number of EVs in the day-ahead operation case. 41
Figure 5.6: Total energy charged and discharged from the power grid and B2B........42
Figure 5.7. Forecasting for the arrivals of customers requesting a certain type of battery. 42
Figure 5.8. RHO scheduling of BSS. 43
Figure 5.9: The profit and the EV arrivals in the RHO operation case study. 43
Figure 5.10: Total energy charged and discharged from the power grid and B2B......44
Figure 5.11. The charging power and energy are stored inside batteries indexed (b=25). 44
Figure 6.1: A sample of the generated PV scenarios for each season 49
Figure 6.2: Scenario reduction for the generated scenarios of PV output power 49
Figure 6.3: The proposed EV arrival rate scenario generation model 50
Figure 6.4: Sample of the scenarios of EV arrivals for weekend and week day. 51
Figure 6.5: Proposed solution approach...56
Figure 6.6: IEEE 38-bus distribution system 58

List of Tables

Table 2.1: Types of EV Charges..22

Table 5.1: Parameters of the BSS Simulation..37

Table 6.1: Data of the BSS 57

Table 6.2: Planning results..59

List of Abbreviations

ACI	Annualized cost of investment
ACK	Acknowledgment
ACM	Annualized cost of maintenance
AR	Annualized revenue
AS	Annualized salaries
ACO	Annualized cost of operation
BSS	Battery Swapping Station
B2G	Battery to Grid
B2B	Battery to Battery
CDF	Cumulative distribution function
CRF	Capital recovery factor
DC	Disposal costs
DB	Depleted Battery
DICDF	Discrete inverse cumulative distribution function
EV	Electric Vehicle
FCS	Fast Charging Station
FCBI	Fully Charged Battery Inventory
G2B	Grid to Battery
LSTM	Long-Short-Term Recurrent Neural Network
LF	Levelization factor
MILP	Mixed Integer Linear Programming
MCS	Monte Carlo Simulation

MCMC	Markov Chain Monte Carlo simulation
PDF	Probability density function
RHO	Rolling Horizon Optimization
RMSE	Root Mean Square Error
RNN	Recurrent Neural Network
SOC	State of Charge
TOU	Time of Use

Nomenclature

A. Sets:

B	Set of batteries.
K	Set of chargers.
T	Set of time slots.
T_{β}^{arv}	A subset of time slots for the EV arrivals at each bay β.
$T_{\beta}^{arv'}$	A complementary subset representing time slots without EV arrivals at each bay β.
$T'_{m,\beta}$	A subset of time slots T representing the time slots with no EV arrivals requesting type *m* batteries at bay β
Tpv	A subset of time slots with PV generation
Tpv'	A subset of time slots without PV generation
U	Set of charging bays.
$\mathcal{B}$	Set of distribution system buses
ψ_m	Group of set B for batteries of type-*m*.
λ_j	Group of set K for chargers group *j*.

B. Parameters:

$\mathrm{c}_{\tau}^{\mathrm{gr}}$	Dynamic grid price in cents per kWh.
$\mathrm{c}^{\mathrm{kWh}}$	Fixed price per kWh swapped
$\mathrm{C}_{b}^{\mathrm{swap}}$	Fixed price in cents for replacing a battery.
$\mathrm{C}^{\mathrm{DEG}}$	Cost of battery degradation
C^{PV}	The cost of charging from the PV system.
cy_{b}	Charging/discharging cycles of each battery.
$\mathrm{DOD}^{\mathrm{max}}$	Maximum depth of battery discharge in %.
d	Discount rate

d'	Effective discount rate
$\mathrm{e}_b^{\mathrm{max}}$	Maximum capacity of battery *b* in kWh.
e	Escalation factor
FF	Fill factor
l_c	Project Life cycle
KI	Current temperature coefficient V/℃
KV	Voltage temperature coefficient A/℃
k	A percentage shaping chargers' characteristics.
$\mathrm{K_m}$	Number of reduced scenarios using k-means
$\mathrm{N}_{\tau,\beta}^{\mathrm{units}}$	The number of batteries requested by an EV.
$\mathrm{N}_{\Omega}^{\mathrm{ch}}$	The number of chargers available in group *j*.
NOCT	Nominal cell operating temperature
N_q	The number of historical data points in each season.
N_{scen}	The number of generated scenarios
n	Number of forecasted data points
$\mathrm{P}_i^{\mathrm{D}}$	The real load demand at bus *i*.
$\mathrm{p}_b^{\mathrm{MAXd}}$	Maximum battery discharging rate in kWh.
$\mathrm{p}_b^{\mathrm{MAXc}}$	Maximum battery charging rate in kWh.
$\mathrm{p}^{\mathrm{GRIDc}}$	The limit for charging power from the grid.
$\mathrm{p}^{\mathrm{GRIDd}}$	The limit for discharging power to the grid.
$\mathrm{P}_\tau^{\mathrm{pv}}$	The output power from the PV system at time τ.
$\mathrm{Q}_i^{\mathrm{D}}$	The reactive load demand at bus *i*.
R_τ	A fraction of the rated load demand at time τ.
r	Number of Multiple random initializations of $\mathrm{K_m}$ centroids
$\mathrm{soc}_{\tau,\beta}^{\mathrm{ev}}$	State Of Charge of the arriving EVs DBs at time τ and bay β.
soc_b^0	Initial SOC of each battery.
$\mathrm{soc}_b^{\mathrm{max}}$	Maximum SOC of any battery 100 %
$\mathrm{V}^{\mathrm{max}}$	The upper bound on the bus voltage.

$V^{\min}$	The lower bound on the bus voltage.
$w_d^{(s)}$	Probability of scenario s
Y	Number of clustered PV output power states
$Y_{i,j}$	The magnitude of the bus admittance matrix.
ζ	A percentage of the maximum battery capacity.
$\Delta soc_b^{\deg}$	Degradation in the battery SOC.
Δt	The time step in hours.
η^{ch}	The efficiency of charging.
η^{dch}	The efficiency of discharging.
$\mu_b^{\deg}$	Battery degradation price.
$\gamma_{i,j}$	The angle of the bus admittance matrix.

C. Variables:

C^{G2B}	Cost of purchasing energy from the grid
$ch_{\tau,b}$	Charging status of battery b at time τ (1 if charging, 0 otherwise).
$dch_{\tau,b}$	Discharging status of battery b at time τ (1 if discharging, 0 otherwise).
F	The total profit of the BSS. (objective function variable)
I_{MPP}	PV cell current at the maximum power point
I_{pv}	PV cell output current
I_{sc}	PV cell short circuit current
$M_{\tau,\beta}$	Decision binary variable for serving an EV at time τ and bay β (1 if served, 0 otherwise)
Ob_h	Observed EV arrivals data point h
Pr_h	Forecasted EV arrivals data point h
$P_{i,\tau}^{BSS}$	The real power injected from the BSS at bus i at time τ.

$p_{\tau,b}^{ch}$	Charging power of any battery b during time slot τ from the power grid.
$p_{\tau,b}^{dch}$	Discharging power of any battery b during time slot τ.
$p_{\tau,b}^{chpv}$	Charging power of any battery b during time slot τ from the PV generation.
$p_{\tau,b}^{grid}$	Injected active power from the main substation in the distribution network
$p_{\tau,b}^{grid}$	Injected reactive power from the main substation in the distribution network
P_{τ}^{loss}	The total power loss in the system due to the loading state at τ.
R^{s}	Revenue from swapping.
R^{B2G}	Revenue from selling energy to the grid.
R^{pv2G}	Revenue from selling excess PV generation to the grid.
S_{IR}	Solar irradiance $Watt/m^2$
$soc_{\tau,b}$	State of charge at the end of time slot τ.
$\Delta soc_{\tau,b}^{swap}$	The difference in SOC between a customers' DB and the swapped charged battery.
$sw_{\tau,b,\beta}$	Swapping status of battery b at time τ and bay β (1 if swapped, 0 otherwise).
T_A	Ambient temperature ℃
T_{cell}	PV cell temperature ℃
$V_{i,\tau}$	The voltage magnitude at bus i at the time τ.
V_{MPP}	PV cell voltage at the maximum power point
V_{oc}	PV cell open-circuit voltage
V_{pv}	PV cell output voltage
$z_{\tau,b}$	Intermediate variable replacing the product of a binary variable and a positive variable.
$\delta_{i,\tau}$	The phase angle at bus i at the loading state τ.

C. Indices:

b	Index of batteries
c	Index of chargers
d	Index of day
i, j	The bus indices
Ω	Index of the group of chargers
k	Index of centroid
l	Index of PV state in the transition matrix
m	Index of battery type
o	Index of PV state in the transition matrix
q	Index of seasons
s	Index of scenario
y	Index of PV output power state
β	Index of swapping bays
τ	Index of time

Chapter 1 . Introduction

In this chapter, we provide a short introduction to Electric Vehicles and their impact on reducing greenhouse emissions. Then, we address the challenges preventing the fast deployment of electric vehicles and how battery swapping stations (BSSs) are a good solution for some of these challenges. Finally, the general organization of the thesis is presented.

1.1. Overview

Due to the advancement in Electric Vehicles (EV) technology and their impact on reducing greenhouse emissions and reliance on fossil fuels, the future of EVs is evolving rapidly. In fact, the number of EVs in the United States is expected to reach 18.7 million by 2030 that is 7% of the expected available vehicles on road in 2030 [1]. Some governments already took actions to revolutionize their roads (e.g., The UK government has launched a plan named 'road to zero' such that all the vehicles on the roads will be zero emissions by 2040 [2]). However, there are still some factors affecting the fast deployment of EVs such as the limited driving range for an EV and the EV charging time. Although few companies started already to produce EVs with an extended driving range (e.g., Tesla Model S 402 miles and Tesla Model 3 322 miles [3]) but this is the official range, however, consumers know that in real-world usage this range is lesser. In this thesis, we deal with the issue of long charging times at EV charging stations. Fast-charging stations (FCSs) would take around 80 minutes to fully charge the Tesla Model S battery [4], whereas it takes only 12 minutes to swap a battery in a typical EV BSS in Shandong province of China [5].

It can be noticed that EV battery swapping stations are being recently introduced in some research papers and the market as well, as it aims to eliminate the EV battery charging times at the charging stations and it's capable of providing grid ancillary services. The BSS concept is based on replacing the depleted battery of the EV owner with a charged battery. The customer's depleted battery is charged at the BSS using DC battery chargers that have less impact on the battery life compared to DC fast chargers. BSSs can provide a swapping service in less than 5 minutes [6].

1.2. Thesis Objectives

Driven by the developing interest in battery swapping stations, and their impact on eliminating the EV charging time, we will focus on designing and planning battery swapping stations. Moreover, we provide a dynamic scheduling model based on a rolling horizon optimization mechanism. The objective of this work is to maximize the daily profit of the BSS considering many factors such as the battery degradation effect, and the battery heterogeneity of different EV types. Additionally, we conduct a set of case studies and sensitivity analyses to prove the model's effectiveness. Finally, a framework is developed for optimal planning of BSSs by optimizing the economic benefits during the station life cycle considering the annualized capital costs, operation costs, and, taking into account the maintenance and recycling costs.

1.3. Research Contribution

The contributions of this research work can be summarized as follows:

- To the best of the author’s knowledge, this is the first model that assesses the BSS optimization problem dynamically using an RHO mechanism while employing a long-short term memory (LSTM) recurrent neural network as a time series forecasting engine to predict the future EVs swapping demand.
- The diversity of the arriving EV type is adopted in this model by introducing multiple units and sizes of batteries. Hence, the BSS can serve an EV requesting single or multiple battery units (e.g. electric buses, trucks, or even large-size electric cars).
- A comprehensive study comparing day-ahead operation and rolling horizon operation versus unscheduled operation is presented in this paper.

1.4. Thesis Organization

The rest of the thesis is organized as follows: Chapter 2 provides background about the BSS technology and recent literature in planning and modeling its operation. Moreover, related works of this research are discussed. The employed methods and algorithms are discussed in Chapter 3 along with the implementation of the proposed approach. Demand forecasting and rolling horizon optimization mechanism are presented in chapter 4. Chapter 5 presents a set of case studies and results analysis for the operational phase. The planning problem formulation and results are presented in chapter 6. Finally, the conclusions are presented in Chapter 7.

Chapter 2 . Background and Literature Review

In this chapter, we discuss the fundamentals and the background behind EVs charging. Then, we present the techniques used for charging EVs at different charging facilities and we focus on explaining the battery swapping station concept and how it provides an alternative for traditional EVs charging. Finally, we discuss the related work in this field of research.

2.1. Background on EVs Charging

There are many different ways to charge an Electric vehicle, in other words, the types of charging stations are categorized into four main categories: residential charging stations, charging while parked at public charging stations, fast-charging stations, and battery swapping stations.

There are 3 main levels for the chargers used at the EV charging stations each has a different charging rating. In Table 2.1 the three main levels for charging are illustrated along with their ratings and the approximate time each charger would take to charge a 24kWh battery. In residential charging, the EVs are recharged usually overnight normally using level-1 chargers which is the slowest way to charge an EV. Whereas charging at public EV charging stations could be faster due to the use of level-2 chargers which are relatively faster. However, FCSs have a very fast charging rate due to the use of fast DC chargers that are capable of charging a 24 kWh battery in about 30 minutes. Finally, battery swapping stations can provide a very fast alternative for charging EVs depleted batteries. The BSS extremely reduces the time of charging EVs similar to that for gasoline refueling of conventional vehicles.

2.1.1. Fast charging stations. Fast charging is also known as rapid charging and it aims to decrease the EV charging time. FCS uses level 3 chargers that are capable to replenish more than 80% of the EV battery capacity in about 20 minutes. Consequently, the traveling range of the EVs is extended if there are FCSs on the way. Although FCS reduced the charging times significantly, it can still have concerns regarding the wait of electric vehicles to charge which might cause traffic jams near the station also fast chargers will significantly reduce the battery lifetime as well. Fast chargers also create an adverse challenge to our power system, namely high current demand and harmonic contamination affecting the peak of our consumption and violating the demand side management.

2.1.2. Battery swapping stations. The BSS concept is based on replacing the depleted batteries (DBs) of the customer's EV with a charged battery. This eliminates the EV charging time and provides a fast reliable swapping service in less than 10 minutes. Figure 2.1 shows the operation principle of the BSS system [7]. Most of the BSSs are designed to trade power with the utility or with microgrids. The BSS sells and purchases energy from the utility based on the dynamic electricity tariff. Such that, the BSS sells power to the grid at high prices and buy power at low prices. Finally, the BSS can be also designed to provide other grid ancillary services e.g. (voltage support and supporting power outages in the power system).

2.2. Related Work

In order to design BSSs and provide optimal operation scheduling for it, an operational model has to be developed to generate profits while meeting the swapping demand. The main idea is to design the BSS station and model its daily operation as in [8]. Furthermore, this could be developed into a planning model over multiple years as

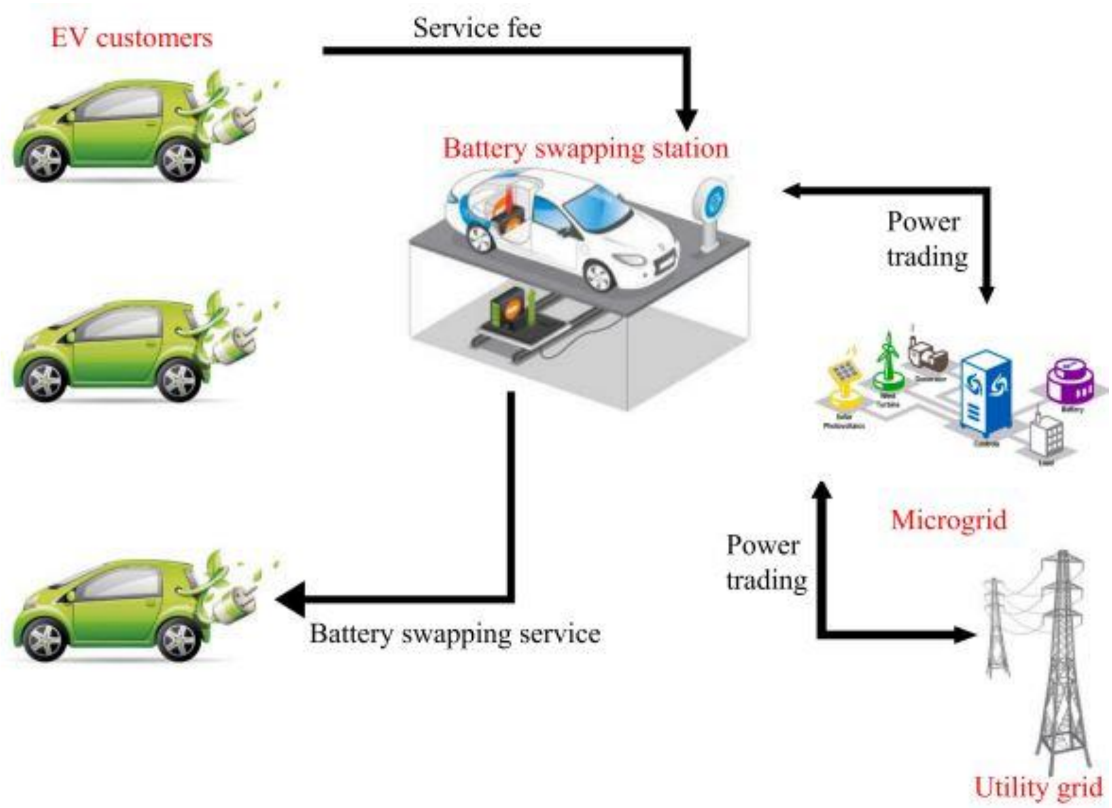

Figure 2.1: The BSS operations [7].

Table 2.1: Types of EV Charges

Charger type	Power supply	Charger power	Charging time (Approx.) for a 24kWh battery
Level-1 (AC charging)	120 VAC 12A to 16 A (single phase)	~1.44kW to ~ 1.92kW	~17 hrs
Level-2 (AC charging)	208 ~ 240VAC 15A ~ 80A (single phase / split phase)	~3.1 kW to ~19.2kW	~8 hrs
Level-3 (DC fast charging)	300 ~ 600VDC Max 400A (polyphase)	~120kW to ~240kW	~30 minutes

in [9]. This can be done typically considering a day-ahead problem where the BSS can take actions considering the dynamic electricity price and the market price as modeled in [10]. Such that, it sells electricity at high prices during the day and purchase it at a low price while meeting the swapping demand. Mostly the optimization problem is based on the fact that charging of the batteries occurs at the BSS station. However, some like Xiaochuan Liu *et al.* combined both operations of BSS and battery charging station, where BSS is only used as a store and depleted batteries are to be charged at battery charging station then delivered to the BSS [11]. However, this would require us to model a transportation system for the batteries and there's no need for it if swapping and charging processes could be done at the same station, which is assumed in this thesis.

2.2.1. BSS with renewable generation and microgrid. Some models considered BSS can run independently if coupled with a micro-grid [12] considering MG and BSS conflicting objectives. Some researchers have studied the operation of BSSs with renewable generation to minimize the costs. Researchers in [13] proposed a BSS coupled with PV generation and the grid considering swapping and PV demand uncertainties. A PV-based BSS is modeled in [14] by considering the service availability and self-consumption of PV. However, these studies ignored the difficulty of installing renewable energy infrastructures in urban cities. Therefore, the proposed model in this thesis will not use any renewable generation to reduce the operating costs. Recently Mingfei Pan incorporated BSS with networked nano-grids [15].

2.2.2. BSSs serving a specific EV type. In [5] an operation model for a BSS serving only electric busses was proposed, whereas in [4] a study has been investigated on a BSS serving electric taxis only in an urban city and it was assumed that most of the stations are operating only from 9.00 a.m. to 8.00 p.m. Hence, the BSS model proposed in this research is operating continuously during the whole day and it's capable of serving any type of electric vehicle.

2.2.3. Variable chargers and battery heterogeneity. While many researchers used a constant charging rate as it's easier to be modeled and reduces the nonlinearity in the model very few researchers used continuously controlled chargers as in [16] which makes it more flexible to provide grid services. Hence, variable chargers are used in this research. In [17] different charging control methods have been proposed considering providing ancillary services to the grid. Very few research works introduced battery heterogeneity into BSSs modeling [18], but they used some impractical assumptions as they require the customers to request battery swapping reservations earlier and specify the battery type and use the expected EV arrival time in their modeling. Thus, we cannot rely on that model in practical operation. In this thesis, a new dynamic operation model for a BSS is proposed which makes it very close to practical operation.

2.2.4. Demand forecasting. There are various research efforts towards determining the Battery swapping demand (e.g. in [10] Robust inventory theory has been used to model the demand uncertainty). Some research work considered the battery swapping uncertainty by modeling the swapping requests probabilistically due to the lack of historical data and the anthropogenic factors in EV arrivals [12]. However in some systems as in [4], the swapping demand could be easily computed since all taxis nearly have the same operation, thus the travel distance and the taxi location are used to predict the swapping demand. Data-driven demand prediction has been subject to research as well. Previous research work as in [5] a backpropagation neural network prediction model is proposed to predict the swapping requests for one day ahead. Also, a wavelet neural network could be used to predict the EV swapping demand [14]. There are also many time series forecasting methods used for predicting the demand for BSSs or EVs charging demand at the parking lot as demonstrated in [19], [20] ARIMA method has been used. Also, time series forecasting using deep learning is one of these methods that could be used for predicting demand for future time steps. It's illustrated in [21] how to forecast time series data using a long short-term memory recurrent neural network (RNN). Unlike convolutional neural networks and backpropagation neural networks, RNN is capable of taking a sequence of data and predicts a future sequence, it has also the capability of updating the network state with the observed values instead of the predicted values [21] – [22].

2.2.5. Solving the optimization problem. BSS Scheduling and operation is formulated as a mixed-integer nonlinear optimization problem. Recently heuristic optimization algorithms have shown good results in solving such problems as shown in [8], [9], and [23]. The authors in [8] integrated algorithm was used to solve the optimization problem for charging schedule for BSS batteries using genetic algorithms, particle swarm optimization, and differential evolution which has proven better results than the typical evolutionary algorithms. In [9] a heuristic technique is used to solve the optimization problem using differential evolution enhanced by fitness sharing which requires less computational time and searches the global optimum more effectively. In [23] a dynamic crossover and adaptive mutation strategy into a hybrid algorithm of particle swarm optimization and genetic algorithm are introduced. However, there's no guarantee that heuristics will result in an optimal solution. Hence, in this model, an exact optimization approach is used. In [10] Mushfiqur R. Sarker represented his problem as a mixed-integer linear programming problem and solved it using CPLEX. Research effort has also been placed to solve large-scale optimization problems that accommodate nonlinearities (e.g. in [16] a generalized benders decomposition algorithm was used to solve the problem such that each sub-problem can be further divided into multiple independent quadratic programming problems.

2.2.6. Rolling horizon predictive scheduling. RHO solves the optimization problem over a moving window which is more robust to uncertainty and better than offline approaches such that it forecasts the arrival of customers with depleted batteries for a future time horizon based on historical data and updates of the actual arrivals at the current time interval. Many researchers have used the online rolling window predictive methods as shown in [24] where a rolling window is used for optimal control of an energy storage unit in a grid-connected microgrid. In [25] an online model predictive controller is demonstrated for a microgrid with plug-in electric vehicles. Also, Alison O'Connell [26] presented a rolling optimization method that focuses on controlling the rate and times at which EVs charge over a 24-h time horizon. On the other hand, the majority of research work related to BSSs preferred modeling the system as a day-ahead problem.

2.2.7. BSS planning. In [9], a proposed study on optimally determining the locations to install BSSs in urban cities, while using a heuristic approach to determine the charging/discharging scheduling of an EV. The problem is modeled as maximizing the net present value of the BSS considering load type, network reinforcement, and reliability analysis. A data-driven approach for solving the BSS location selection problem to satisfy the battery swapping demand of EVs was investigated in [27] while using large-scale GPS data from taxis and electricity requests. Some researchers as Qi Kang introduced a centralized charging strategy of EVs under a battery swapping scenario considering optimal charging priority and charging location (station or bus node in a power system) based on spot electric price [23]. Similarly in [28], the authors introduced a centralized solution for an optimal scheduling problem for battery swapping that assigns to each EV a best based on the station location and the SOC while considering EV range constraints, grid operational constraints, and ac power flow equations and assuming that distribution grid, battery stations, and EVs are managed centrally by the same operator. In [29] the same case in [28] was investigated but with a distributed solution such that the distribution grid, stations, and EVs are managed by separate entities. Since BSS is an emerging technology most of the literature work disregarded many factors such as queuing analysis, battery heterogeneity, and the diversity of arriving EV type (e.g. Electric cars, Taxis, Busses, and trucks). The queuing analysis is a very important factor for estimating the queue length and waiting time and essential part of planning and sizing of battery swapping stations. However, queuing analysis has been widely adopted in research articles related to fast-charging stations [30]-[32].

Chapter 3 . Methodology

In this chapter, a general framework of the proposed BSS is presented. The assumptions used in modeling the BSS are highlighted. We also formulate a mathematical model for the BSS operations.

3.1. The Structure of the Proposed BSS System

A general framework of the proposed BSS is illustrated in Figure 3.1. as it shows that the BSS consists of five main parts, namely, i) The power system, ii) The charging partition, iii) The fully charged battery inventory (FCBI), iv) The swapping bays, v) The BSS control center.

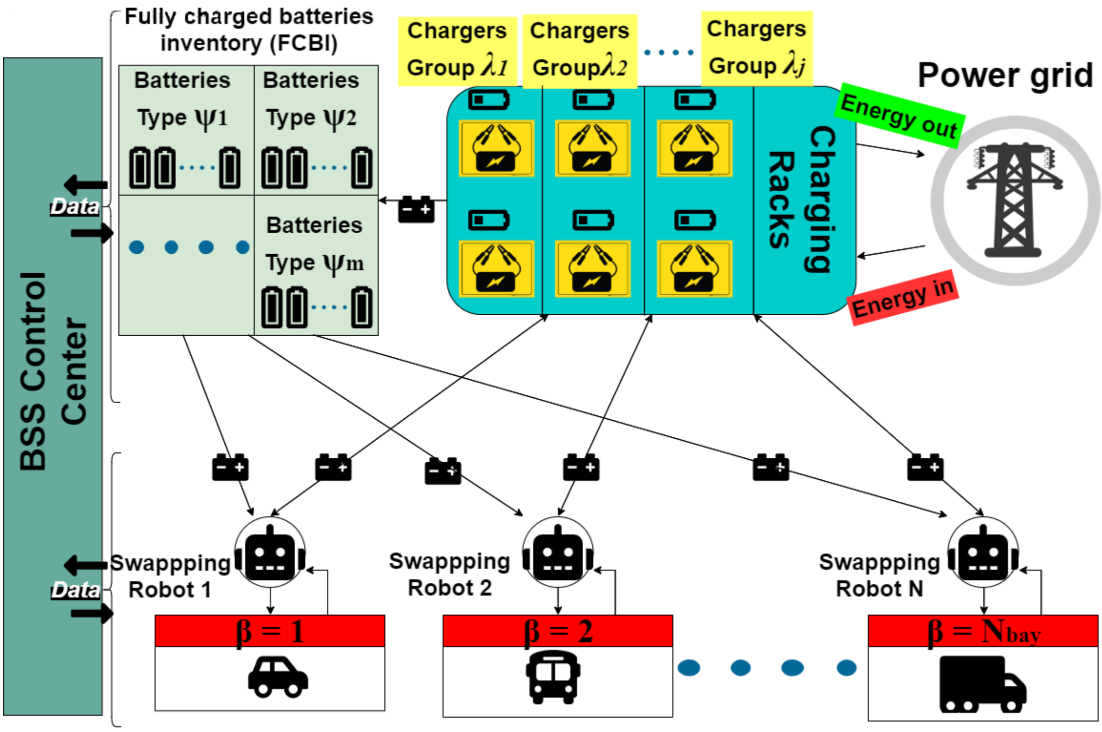

Figure 3.1: The structure of the proposed BSS model.

3.1.1. Details of the system model. In this model, a fully automated swapping system using robots is proposed. Once a battery is fully charged it's automatically transferred to the FCBI. The BSS model is mainly providing service to EVs by unloading the DBs from the arriving EV and replacing it with a fully charged one from the FCBI or a partially charged battery from the charging racks. The minimum SOC of a partially charged battery cannot be less than a certain Threshold (ζ). Our BSS consists of several swapping bays for EVs requesting single battery units, while some other bays are used to serve EVs requesting more than one battery unit (e.g. Electric busses or trucks). Meanwhile, the BSS has a heterogeneous battery stock that contains different battery types for serving different types of EVs. Since different types of batteries can vary greatly due to different manufacturers and models, also to avoid problems such as compatibility which is one of the concerns for lithium-ion batteries the BSS has different groups of DC chargers each is specified for a certain type of battery. These chargers are advanced chargers that could charge/discharge with a continuously controlled power to get more flexibility while supplying energy to the grid. Hence, fully utilize the battery-to-grid (B2G), grid-to-battery (G2B), and battery-to-battery (B2B) concepts and efficiently provide grid ancillary services. The BSS has a control center that is responsible for providing an optimal schedule for charging/discharging/swapping processes at the BSS, while continuously monitoring and predicting the BSS demand, number of charged batteries in stock, and the SOC of the batteries, and the dynamic price of electricity.

3.1.2. Assumptions. It is assumed that batteries are owned by the BSS so that it's responsible for its charging/discharging, state of health, and degradation. There must be a contract between the BSS operator and the customers including that customers are not allowed to charge the battery elsewhere and return it for swapping at the BSS before a certain date. A heterogeneous battery inventory is proposed for serving different EV models from different manufacturers. It's also assumed that different EV types for a certain manufacturer (e.g. cars, buses, or trucks) can use single or multiple units of a unified battery type. The SOC of a customer's DB cannot go below a certain minimum value. Meanwhile, the SOC of a charged battery swapped to a customer should not less be than a certain threshold. A fully automated swapping system is assumed with a proposed swapping service under 10 minutes. All data such as EV actual arrivals, SOC of the DBs, and SOC of each battery at the charging racks and the number of fully charged batteries in stock are obtained and transferred immediately to the BSS control center to set the scheduling actions.

3.2. Optimization Model

The proposed optimization model is based on an RHO mechanism which is later explained in chapter 4. Such that the BSS control center predicts the EV arrivals for an upcoming time horizon and optimization takes place based on the predicted arrivals. Thus, charging /discharging and swapping schedules are to be optimally acquired.

3.2.1. The BSS mathematical model. The optimization model is given in (1-28) for batteries $b \in B = \{1,2,\dots,\mathrm{N}^{\mathrm{bat}}\}$, swapping bays $\beta \in U = \{1,2,\dots,\mathrm{N}^{\mathrm{bay}}\}$, chargers $c \in K = \{1,2,\dots,\mathrm{N}^{\mathrm{ch}}\}$, type of batteries $\psi = \{\psi_1, \psi_2, \dots, \psi_m\}$, and a group of chargers $\lambda = \{\lambda_1, \lambda_2, \dots, \lambda_\Omega\}$. Where $[\psi_1 \cup \psi_2 \cup \dots \cup \psi_m = B]$, $[\psi_1 \cap \psi_2 \cap \dots \cap \psi_m = \{\phi\}]$, $[\lambda_1 \cup \lambda_2 \cup \dots \cup \lambda_\Omega = K]$,$[\lambda_1 \cap \lambda_2 \cap \dots \cap \lambda_\Omega = \{\phi\}]$; where *m* and *j* are the indices of battery types and charger groups available at the BSS respectively. A group of chargers has chargers of the same type and characteristics. Each group of chargers is assigned to a certain battery type. In the following formulation chargers group, λ_j is assigned to battery type ψ_m, $\forall(m = \Omega)$. The number of chargers in each group Ω is $\mathrm{N}_\Omega^{\mathrm{ch}}$. In the objective function (3.1), the profit of the BSS during a certain time interval is represented as the submission of the revenue from the battery swapping to the customers and the revenue from selling energy to the grid and deducting the costs which are mainly the cost of energy purchased from the grid to charge the batteries and the battery degradation cost.

$$\max_F = R^s + R^{B2G} - C^{G2B} - \mathrm{C}^{\mathrm{DEG}} \tag{3.1}$$

$$\left.\begin{aligned} R^s = &\sum_{(\tau\in T)} \sum_{(b\in B)} \sum_{(\beta\in U)} sw_{\tau,b,\beta} \times \mathrm{c}_b^{\mathrm{swap}} \\ &+ \sum_{(\tau\in T)} \sum_{(b\in B)} \frac{e^{max}{}_b}{100} \times \Delta soc_{\tau,b}^{swap} \times \mathrm{c}^{\mathrm{kWh}} \end{aligned}\right\} \tag{3.2}$$

$$R^{B2G} = \sum_{(\tau\in T)} \sum_{(b\in B)} \Delta\mathrm{t} \times \mathrm{c}_\tau^{\mathrm{gr}} \left(\eta^{\mathrm{dch}} \times p_{\tau,b}^{dch}\right) \tag{3.3}$$

$$C^{G2B} = \sum_{(\tau\in T)} \sum_{(b\in B)} \Delta\mathrm{t} \times \mathrm{c}_\tau^{\mathrm{gr}} \left(\frac{p_{\tau,b}^{ch}}{\eta^{\mathrm{ch}}}\right) \tag{3.4}$$

Subject to:

$$\Delta soc_{\tau,b}^{swap} = \sum_{(\beta\in U)} \left(soc_{\tau-1,b} - \mathrm{soc}_{\tau,\beta}^{\mathrm{ev}}\right) \times sw_{\tau,b,\beta} \qquad \forall(\tau \geq 2) \in T, \forall\, b \in B, \tag{3.5}$$

$$\Delta soc_{\tau,b}^{swap} = \sum_{(\beta\in U)} \left(\mathrm{soc}_b^0 - \mathrm{soc}_{\tau,\beta}^{\mathrm{ev}}\right) \times sw_{\tau,b,\beta} \qquad (\tau = 1) \in T, \forall\, b \in B, \tag{3.6}$$

$$ch_{\tau,b} + \sum_{(\beta \in U)} sw_{\tau,b,\beta} \ \leq 1 \qquad \forall \tau \in T, \forall\, b \in B, \tag{3.7}$$

$$soc_{\tau,b} = soc_{\tau-1,b} + \frac{\left(p_{\tau,b}^{ch} - p_{\tau,b}^{dch}\ \right) \times \Delta \mathrm{t}}{\mathrm{e}_b^{\max}} \times 100 - \Delta soc_{\tau,b}^{swap} \qquad \forall (\tau \geq 2) \in T, \forall\, b \in B, \tag{3.8}$$

$$soc_{\tau,b} = \mathrm{soc}_b^0 + \frac{\left(p_{\tau,b}^{ch} - p_{\tau,b}^{dch}\ \right) \times \Delta \mathrm{t}}{\mathrm{e}_b^{\max}} \times 100 - \Delta soc_{\tau,b}^{swap} \qquad (\tau = 1) \in T, \forall\, b \in B, \tag{3.9}$$

$$(\mathrm{soc}_b^{max} - \mathrm{DOD}^{\max}) \leq\ soc_{\tau,b} \leq \mathrm{soc}_b^{max} \qquad \forall \tau \in T, \forall\, b \in B, \tag{3.10}$$

$$soc_{\tau-1,b}\ \geq \zeta \times \sum_{(\beta \in \mathrm{U})} sw_{\tau,b,\beta} \qquad \forall (\tau \geq 2) \in T, \forall\, b \in B, \tag{3.11}$$

$$\mathrm{soc}_b^0\ \geq \zeta \times \sum_{(\beta \in U)} sw_{\tau,b,\beta} \qquad (\tau = 1) \in T, \forall\, b \in B, \tag{3.12}$$

The decision variable vector $F = \left(p_{\tau,b}^{ch}, p_{\tau,b}^{dch}, ch_{\tau,b}, sw_{\tau,b,\beta}\right)^T$ includes the variables for batteries charging/discharging and swapping processes. In (3.2) the binary variable $sw_{\tau,b,\beta}$ represents the status of the battery b at any time τ at any swapping bay β such that it's 1 if a battery is swapped at a certain bay at the end of time slot τ and 0 otherwise. Meanwhile, the revenue from swapping is represented as submission of two terms a) fixed price per replacement of a battery unit b) revenue per kWh replaced to customers. In (3.3) & (3.4) the price of energy charged/discharged from the grid is calculated based on TOU. Equations (3.5) & (3.6) calculate the drop in the SOC of a certain battery b if it's replaced by a DB arriving with $\mathrm{soc}_{\tau,\mathrm{b}}^{\mathrm{ev}}$ at any time τ. If a battery b is not swapped at any swapping bay β at time τ, therefore, the variables $sw_{\tau,b,\beta}$ & $\Delta soc_{\tau,b}^{swap}$ are 0. Constraint (3.7) states that any battery at any time τ is either swapped at any swapping bay β if $sw_{\tau,b,\beta}$ is 1 or charging at the charging racks if the binary variable $ch_{t,b}$ is 1, thus both charging and swapping processes cannot occur at the same time for the same battery. It also ensures that a certain battery b cannot be replaced at two different swapping bays at the same time slot. In (3.8) & (3.9) the state of charge of each battery b at any time τ is calculated while taking the SOC at the previous time slot τ-1, charging and discharging power efficiencies η^{c} & η^{d} into consideration. The

SOC of any battery in the BSS cannot be discharged less than the DOD^{max} and cannot exceed soc_b^{max} as shown in (3.10). Equation (3.11) provides the option for swapping partially charged batteries from the charging racks as it states that any battery is eligible to be swapped to a customer at any bay if it maintains a SOC above a certain threshold such that if a customer arrives at a time τ the SOC at time τ -1 of the charged battery has to be above a certain Threshold (ζ). This provides a more flexible service as not only FBs from the inventory are swapped but also partially charged ones. Similarly, equation (3.12) ensures maintaining an initial soc_b^0 for any battery above a certain threshold at the beginning of the day if this battery is to be replaced at the end of the first time slot (τ = 1).

$$\sum_{(b \in B)} sw_{\tau,b,\beta} = \mathrm{N}_{\tau,\beta}^{\mathrm{units}} \times M_{\tau,\beta} \qquad \forall t \in T_\beta^{arv}, \forall\, \beta \in U, \tag{3.13}$$

$$sw_{t,b,\beta} = 0 \qquad \forall \tau \in T_\beta^{arv'}, \forall\, b \in B, \forall\, \beta \in U, \tag{3.14}$$

At any time slot τ at the same bay β only one customer can swap a single or multiple battery unit(s). The customer also swaps a specific battery type for his EV from the types offered by the BSS as shown later in (3.20). Constraint (3.13) states that EVs arriving at bay β at time τ requesting $\mathrm{N}_{\tau,\beta}^{\mathrm{units}}$ units of batteries for swapping could be served or not; where $M_{\tau,\beta}$ is a binary variable equal to 1 if the EV is served and 0 otherwise. Whereas equation (3.14) fixes the $sw_{\tau,b,\beta}$ variable to zero at any bay β at the time slots $T_\beta^{arv'}$ at that bay.

$$0 \le p_{\tau,b}^{ch} \le \left(\mathrm{p}_c^{\mathrm{MAXc}} \times e^{\frac{\mathrm{k} - soc_{t,b}}{\mathrm{P}_c^{\mathrm{MAXc}}}} \right) \times ch_{\tau,b} \tag{3.15}$$

$$\forall \tau \in T \;\; \forall b \in \psi_m \;\; \forall c \in \lambda_\Omega \;\; \forall (m = \Omega) \in \psi,$$

$$0 \le p_{\tau,b}^{ch} \le \mathrm{p}_c^{\mathrm{MAXc}} \times ch_{\tau,b} \tag{3.16}$$

$$\forall \tau \in T \;\; \forall b \in \psi_m \;\; \forall c \in \lambda_\Omega \;\; \forall (m = \Omega) \in \psi,$$

$$0 \le p_{\tau,b}^{dch} \le \mathrm{p}_c^{\mathrm{MAXd}} \times ch_{\tau,b} \tag{3.17}$$

$$\forall \tau \in T \;\; \forall b \in \psi_m \;\; \forall c \in \lambda_\Omega \;\; \forall (m = \Omega) \in \psi\,,$$

$$\sum_{(b \in B)} p_{\tau,b}^{ch} \le \mathrm{p}^{\mathrm{GRIDc}} \tag{3.18}$$

$$\forall \tau \in T,$$

$$\sum_{(b \in B)} p_{\tau,b}^{dch} \leq \mathrm{p}^{\mathrm{GRIDd}} \qquad \forall \tau \in T, \tag{3.19}$$

To fully utilize the benefits from the grid services variable rate chargers were used rather than the constant current chargers that are controlled by simple on/off control methods. The combination of constraints (3.15) and (3.16) shapes the variable charger characteristics as they define the bounds on the charging power. The variable charging characteristics are modeled as a function of the battery SOC as it decreases exponentially less than $\mathrm{p}_c^{\mathrm{MAXc}}$ when the SOC exceeds a certain k% as shown in (3.15). In (3.17) a battery could only be discharged at the rated power $\mathrm{p}_c^{\mathrm{MAXd}}$. The parameters $\mathrm{p}_c^{\mathrm{MAXc}}$ and $\mathrm{p}_c^{\mathrm{MAXd}}$ are set according to the group of chargers λ_j assigned to each battery type ψ_m; recall, in this model, we assign $(m = \Omega)$. Constraints (3.18) & (3.19) represent the upper bound and lower bound on the total power charged/discharged from the grid at time τ.

3.2.2. Battery heterogeneity. The proposed BSS framework introduces battery heterogeneity to get a realistic model for real BSS operation. Equation (3.20) use the subset of time slots $T'_{m,\beta}$ when there's no EV arrival requesting battery type ψ_m at bay β and prevents swapping charged batteries of this type ψ_m by setting $sw_{\tau,b,\beta} = 0$ at these time slots. Due to the different types of batteries available, each type ψ_m is assigned for a group of chargers λ_j, where (*m*=*j*). In (3.21) the total number of batteries of a certain type ψ_m that can be charging at the same time are restricted to the number of chargers $\mathrm{N}_j^{\mathrm{ch}}$ in group λ_j assigned to this type.

$$sw_{\tau,b,\beta} = 0 \qquad \forall \tau \in T'_{m,\beta}\ \forall\, b \in \psi_m\ \ \forall m \in \psi\ \ \forall\, \beta \in U, \tag{3.20}$$

$$\sum_{(b \in \psi_m)} ch_{\tau,b} \leq \mathrm{N}_{\Omega}^{\mathrm{ch}} \qquad \forall \tau \in T\ \ \forall (m = \Omega) \in \psi, \tag{3.21}$$

3.2.3. Battery degradation effect. The batteries in the BSS undergo many charging/discharging cycles, which reduce the battery lifetime and result in decreasing the maximum capacity of the battery. In this model battery characteristics is highly dependent on the number of cycles, as illustrated in [26], however, other battery chemistries are highly sensitive to the $\mathrm{DOD}^{\max}$ [27]. The degradation in a certain battery SOC is calculated in (3.22) as a function of the number of cycles. The degradation effect is added to the formulation by subtracting the degradation cost from the total revenue as shown in (3.1). Equation (3.23) calculates the degradation cost for all the batteries available at the BSS.

$$\Delta \mathrm{soc}_b^{\mathrm{deg}} = -8.954 \times 10^{-10} \times \mathrm{cy}_b^3 + 7.883 \times 10^{-7} \times \mathrm{cy}_b^2 - 2.814 \times 10^{-4} \times \mathrm{cy}_b \qquad \forall b \in B. \tag{3.22}$$

$$\mathrm{C}^{\mathrm{DEG}} = \sum_{(b \in B)} 100\,\% \times \Delta \mathrm{soc}_b^{\mathrm{deg}} \times \mu_b^{\mathrm{deg}} \tag{3.23}$$

3.2.3. Linearization. To deal with run time issues some equations are to be linearized. In (3.5) the term $soc_{\tau-1,b} \times sw_{\tau,b,\beta} = 0$ is nonlinear so in order to linearize this equation it is replaced by equations (3.24)-(3.27), such that the nonlinear term is replaced by a positive variable $z_{t,b}$ which equals to $soc_{\tau-1,b}$ from equations (3.26)&(3.27) if $sw_{\tau,b,\beta} = 1$. If $sw_{\tau,b,\beta} = 0$ variable $z_{\tau,b}$ is forced to 0 in (3.25) & (3.26) since it's a positive variable.

$$\Delta soc_{\tau,b}^{swap} = \sum_{(\beta \in U)} \left(z_{\tau,b} - \mathrm{soc}_{\tau,\beta}^{\mathrm{ev}} \times sw_{\tau,b,\beta} \right) \qquad \forall (\tau \geq 2) \in T, \forall\, b \in B, \tag{3.24}$$

$$z_{\tau,b} \leq sw_{\tau,b,\beta} \times \mathrm{soc}_b^{max} \qquad \forall \tau \in T_\beta^{arr}, \forall\, b \in B, \forall\, \beta \in U, \tag{3.25}$$

$$z_{\tau,b} \geq soc_{\tau-1,b} - (1 - sw_{\tau,b,\beta}) \times \mathrm{soc}_b^{max} \qquad \forall (\tau \geq 2) \in T, \forall\, b \in B, \forall\, \beta \in U, \tag{3.26}$$

$$z_{\tau,b} \leq soc_{\tau-1,b} \qquad \forall (\tau \geq 2) \in T, \forall\, b \in B, \forall\, \beta \in U, \tag{3.27}$$

$$p_{\tau,b}^{C} \leq -\alpha soc_{\tau,b} + \gamma \qquad \forall \tau \in T, \forall b \in B, \tag{3.28}$$

Chapter 4 . Demand Forecasting

In this chapter, we present a dynamic optimal operation mechanism for the BSS. We deal with the optimization problem in a dynamic manner using a rolling horizon predictive controller. Moreover, we employ the long-short term memory recurrent neural network which is a deep learning technique used as a time series forecasting engine to forecast the EV arrivals.

4.1. Rolling Horizon Predictive Controller

The idea of rolling horizon optimization is to consider forecasted data over a limited horizon in addition to the currently available information to develop the optimal decisions. The rolling horizon mechanism can be implemented by defining three horizons—namely, the scheduling horizon, the control horizon ($\boldsymbol{C}$), and the forecasting horizon ($\boldsymbol{u}$) [28]. For a BSS, at each time slot τ, the optimization model considers the current EV arrivals at the control horizon and the forecasted arrivals at future time slots $\tau + \boldsymbol{u}$ over the scheduling period T where $1 \le \boldsymbol{u} \le N_T - 1$; N_T is the number of time slots in the scheduling horizon.

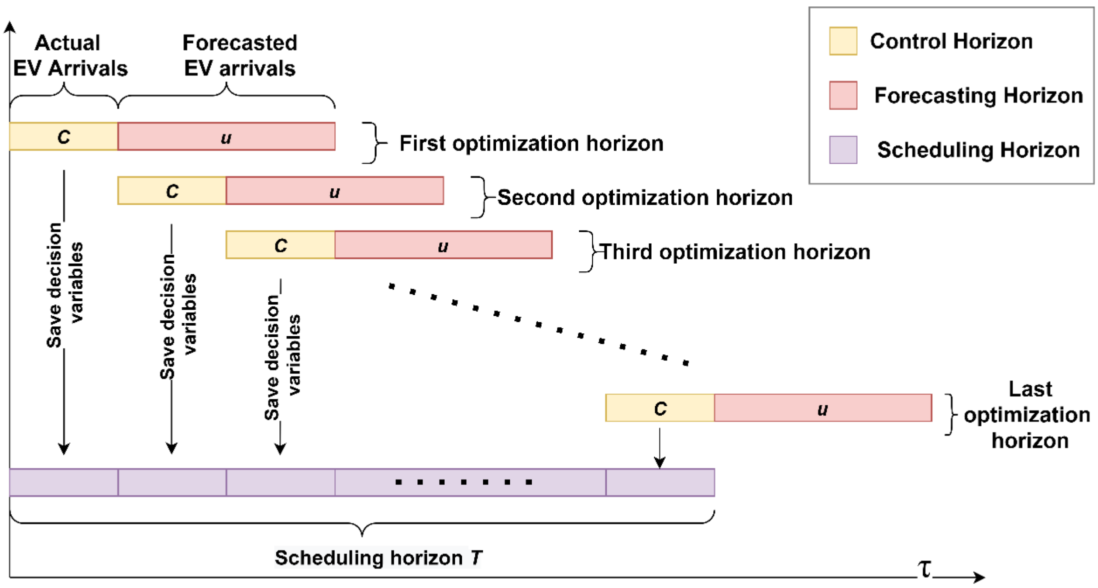

Figure 4.1: Rolling horizon mechanism

The optimized scheduling for the whole day is done after the rolling horizon keeps rolling till reaching the last time slot in the day as clarified in Figure 4.1 The rolling horizon mechanism can be implemented as follows:

- Start by initializing the system and specifying the length of the scheduling horizon, the control horizon, and the forecasting horizon.
- Execute the first optimization interval and solve the scheduling problem.
- Save the decisions and the variables of the control horizon to be used as initial conditions for the following optimization interval.
- Start the following optimization interval after updating the control horizon and the forecasting horizon.
- Keep looping until the new schedule corresponds to the last time slot of the day.

4.2. LSTM for Forecasting

To forecast the number of customers arriving and the type of requested battery(s) at each time slot RNNs is an efficient time series forecasting engine that allows feeding values forward in time since it uses not only the input data but also the previous outputs for making the current prediction. However, it's very hard to train and forgettable so we used an evolution of RNN which was introduced by Hochreiter and Schmidhuber [33]. This network has a gated memory unit for neural networks and it is capable of learning long-term dependencies and remembering information for long periods. The LSTM structure shown in Figure 4.2 has memory blocks called cells and it has 3 gates managing the memory contents each gate is a logistic function with weighted sums. Equations (4.1), (4.2), and (4.3) represent the forget gate, input gate, and output gate respectively, and the sigmoid function in each decides about the data that will be omitted from each cell. The input gate decides which new inputs flow into the cell state, the forget gate determines which values from the old output to forget and which values remain by looking at the current input (X_τ) and the previous output ($h_{\tau-1}$) and the output gate decides about values to be executed. Equation (4.4) is responsible for updating the current cell state which is equal to the values omitted from the previous cell state plus the new candidate values entering the cell state. The output values from the output gate are enhanced and produced in a filtered version as shown in (4.5). The root mean squared error (RMSE) is commonly used as an evaluation for the forecasting performance as it compares the predicted values with the actual observed values. In equation (4.6) the RMSE is calculated, where Ob_i & Pr_i are observed and predicted EV arrivals respectively. The framework combining LSTM with the RHO is further detailed in lines 1-13 in Algorithm 1. where b_i, b_f, b_o& b_c are bias, and W_i, W_f, W_o& W_c represent weight matrices.

Algorithm 1: Pseudo code for the RHO and LSTM

Input: Historical EV arrivals data and current EV arrivals

Output: RHO scheduling for the BSS operations

Initialize $\boldsymbol{C}$, $\boldsymbol{u}$, N_T, and the length of the LSTM training set (Q)

1: **for** τ = 1: ($N_T - 1$) **do**

2: Update the system state with the EV arrivals N_τ^{arr} in $\boldsymbol{C}$

3: LSTM Forecasting for the interval $\tau + \boldsymbol{u}$:

4: Data preprocessing (e.g. normalize the training set)

5 Create the input sequence and train LSTM:

6: X^T={$X_{\tau-Q}$, ⋯,$X_{\tau-2}$, $X_{\tau-1}$}={$N_{\tau-Q}^{arr}$, ⋯ , $N_{\tau-2}^{arr}$, $N_{\tau-1}^{arr}$}

7: Predict output sequence $O \longleftarrow$ LSTM(X):

8: O^T = {N_τ^{arr}, $N_{\tau+1}^{arr}$, ⋯ , $N_{\tau+\boldsymbol{u}}^{arr}$} = {$O_\tau$, $O_{\tau+1}$ ⋯ , $O_{\tau+\boldsymbol{u}}$}

9: Evaluate the forecasting performance using RMSE

10: Update the training interval $Q \coloneqq Q + \boldsymbol{C}$

11: Run BSS scheduling model over the horizon $\boldsymbol{C} + \boldsymbol{u}$

12: Save the decision variables F for the period $\boldsymbol{C}$

13: **end for**

$$f_\tau = \sigma\left(W_f \times +U_f \times h_{\tau-1} + b_f\right) \tag{4.1}$$

$$i_\tau = \sigma(W_i \times X_\tau + U_i \times h_{\tau-1} + b_i) \tag{4.2}$$

$$O_\tau = \sigma(W_o \times X_\tau + U_o \times h_{\tau-1} + b_o) \tag{4.3}$$

$$C_\tau = f_\tau \times C_{\tau-1} + i_\tau \times tanh(W_c \times X_\tau + U_c \times h_{\tau-1} + b_c) \tag{4.4}$$

$$h_\tau = O_\tau \times tanh(C_\tau) \tag{4.5}$$

$$RMSE = \sqrt{\frac{1}{n}\sum_{h=1}^{n}(Ob_h - Pr_h)^2} \tag{4.6}$$

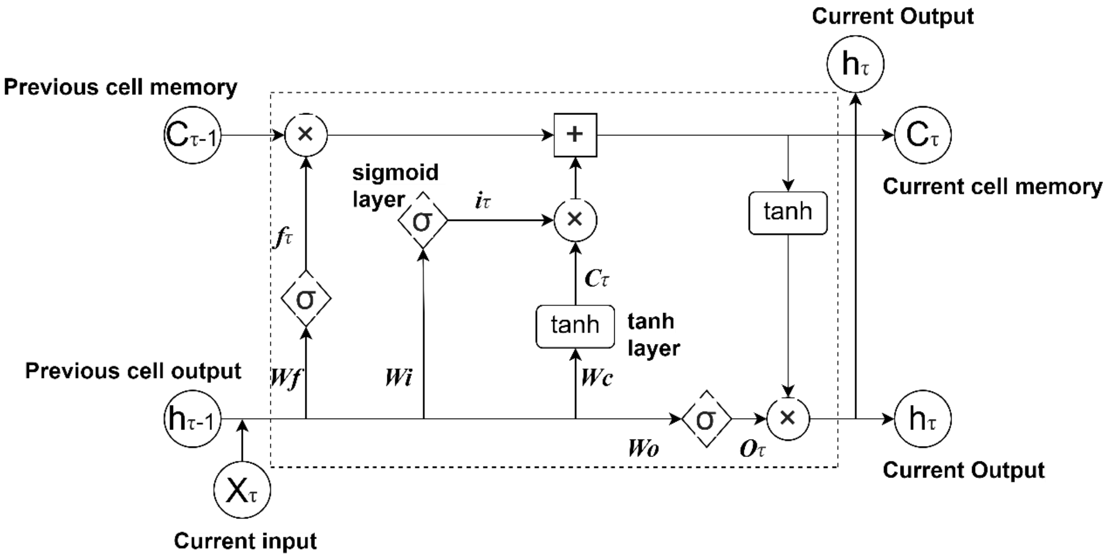

Figure 4.2: The LSTM cell structure

Chapter 5 . Operation Case Studies and Simulation

This chapter carries out a set of case studies to show the effectiveness of the RHO mechanism and comparing optimization results versus unscheduled operation and day-ahead scheduling of the BSS. The model is defined as a MILP and it's implemented in GAMS 30.3.0 and solved using CPLEX solver [34].

Table 5.1: Parameters of the BSS Simulation

Parameters	Value
$b \in \psi_1$ indices	(b = [1-30])
$b \in \psi_2$ indices	(b = [31-60])
$\mathrm{c}_b^{\mathrm{swap}}$	500 ¢ if $b \in \psi_1$, 1200 ¢ if $b \in \psi_2$
$\mathrm{c}^{\mathrm{kWh}}$	50 ¢/kWh
$\mathrm{DOD}^{\max}$	80%
$\mathrm{e^{max}}_b$	16 kWh if $b \in \psi_1$, 42 kWh if $b \in \psi_2$
k	70%
N^{ch}	26; $\mathrm{N}_1^{\mathrm{ch}} = \mathrm{N}_2^{\mathrm{ch}}$=13
No. of batteries ($\mathrm{N}^{\mathrm{batt}}$)	60; 30 of type ψ_1+30 of type ψ_2
No. of bays ($\mathrm{N}^{\mathrm{bay}}$)	3
No. of EV arrivals	150
$\mathrm{p}_c^{\mathrm{MAXc}}$, $\mathrm{p}_c^{\mathrm{MAXc}}$	8 kW if $c \in \lambda_1$, 25 kW if $c \in \lambda_2$.
Batteries of type ψ_1	Charged with chargers group $c \in \lambda_1$
Batteries of type ψ_2	Charged with chargers group $c \in \lambda_2$
$\mathrm{p}^{\mathrm{GRIDc}}$, $\mathrm{p}^{\mathrm{GRIDd}}$	429 kW
soc_b^0	100 %
ζ	90 %
$\Delta\mathrm{t}$	1/6
η^{ch}, η^{dch}	0.94
μ_b^{deg}	40 ¢

The LSTM forecasting is implemented in MATLAB [35]. The swapping service is provided within 10 minutes. Thus the simulation is tested over the 24 hours of the day equivalent to 144-time slots each is 10 minutes.

Table 5.1 defines the parameters used in the simulation. The parameters are mainly the prices of the swapping service, the operation costs, and limitations on charging/discharging, and limitations on the power exchange with the power grid. The actual EV arrivals can be shown in Figure 5.4 and the grid TOU price can be shown in Figure 5.6.

5.1. Case Study I (Day-Ahead Scheduling for a Small Battery Stock)

This is an illustrative case study to validate the optimization model and to ensure meeting the constraints in section III. The same values of the parameters from Table 5.1 are used. However, for simplicity, the number of batteries is reduced to three units: two of type ψ_1 and one type ψ_2. Also, only 1 charger for each battery type is used. Six customers arrived at different swapping bays at different time slots of the day. EVs requesting more than one battery unit arrive at bay (β = 3) in all case studies and represented by a black square or circle. In Figure 5.1, batteries with indices *(b* = 1 & 2) are of type ψ_1, whereas batteries with index (b = 3) are of type ψ_2. Day-ahead scheduling applied to the EV arrivals profile in Figure 5.1. In day-ahead scheduling, it is assumed that the day starts and ends with charged batteries equal to or above 90% SOC. Therefore constraint (4.6) is added for charging the batteries at the end of the day to 90% or above. Thus, ensuring batteries are charged before the beginning of the next day.

In Figure 5.1, the sudden drop in a certain battery SOC indicates swapping this battery with the depleted one of the arriving EVs. In all the case studies, the EV arrivals point highlighted in yellow represent served customers. EVs arriving at 4:10 AM and 5:50 AM request type ψ_2 batteries and it can be seen that only batteries with index (b=3) swapped. Whereas, the rest of EVs arrivals request type ψ_1 batteries and could only be swapped with batteries (b = 1 & 2) It can be observed that the SOC of batteries swapped at any time τ is equal to or above the threshold (ζ = 90%) at the end of time slot τ-1 before swapping. Since there's only one charger available for type ψ_1 batteries, therefore b = 1 & 2 cannot be charging at the same time; one is charging while the other is constant and vice-versa. The large EV arriving at 4:50 PM requests 2 battery units of

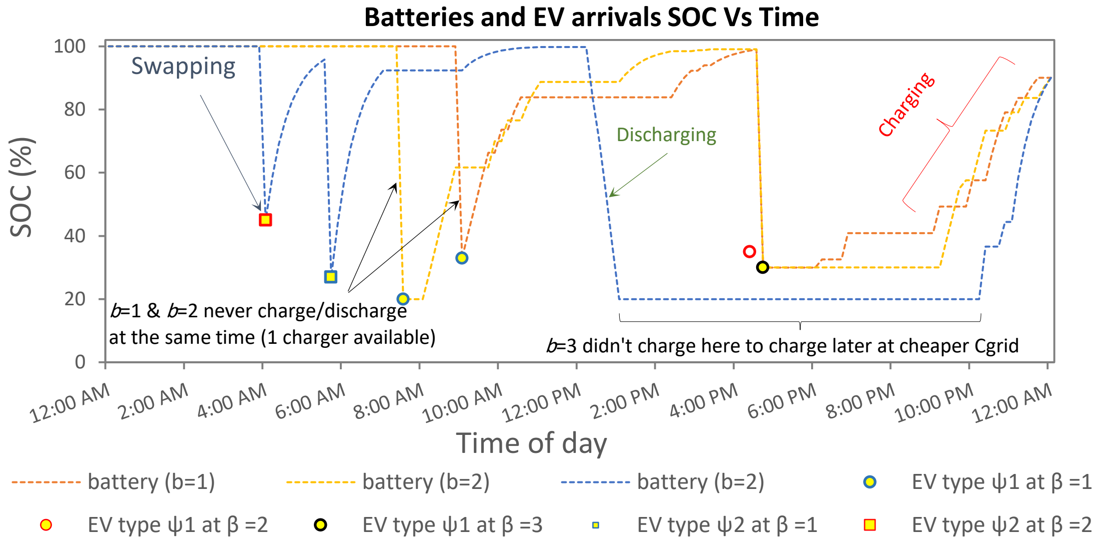

Figure 5.1: Day-ahead scheduling for a small battery stock.

type ψ_1, thus the optimization favored swapping 2 units to this customer and rejected the customer requesting one unit at 4:30 PM.

$$soc_{\tau=144,b} \geq 90 \qquad \forall\, b \in B. \tag{5.1}$$

5.2. Case Study II (Unscheduled Operation)

This case study represents the base case for a BSS operating without optimization. The idea is mainly based on serving a customer and swapping his DB if there's an available charged battery otherwise batteries are either charging or stored at

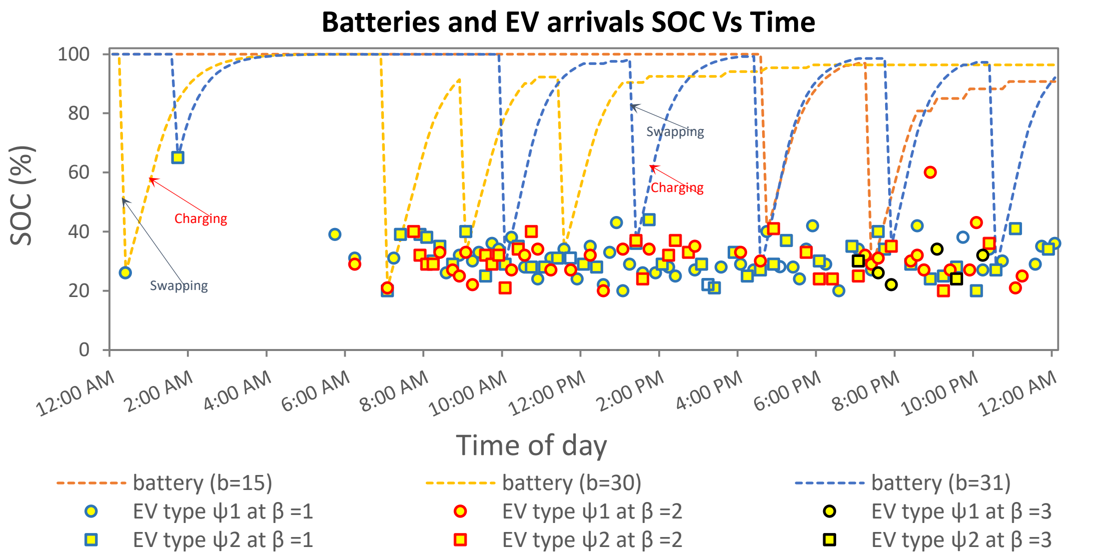

Figure 5.2. Unscheduled operation of BSS while charging as soon as possible

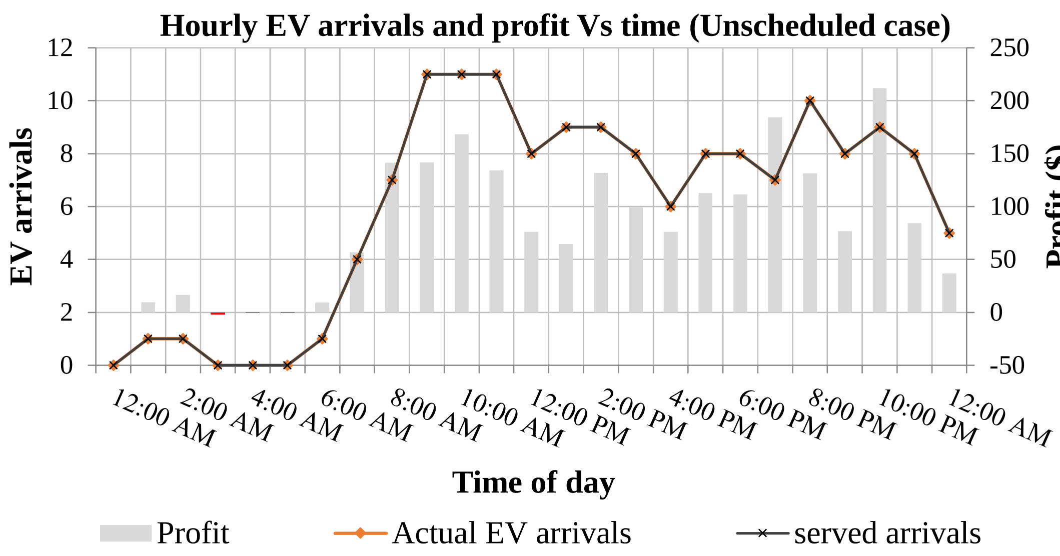

Figure 5.3: The profit and the number of EV arrivals in the unscheduled operation.

the FCBI. The parameters in Table 5.1 are used in this case study. Figure 5.2 shows the SOC for a sample of three batteries during the day. For comparison, the EV arrivals used in this case are the same actual EV arrivals in case-D. This unscheduled operation case is defined as charging as soon as possible to serve more customers while excluding discharging to the grid. It's considered a greedy algorithm as DBs are immediately charged after swapping as shown in Figure 5.2 to serve more customers. The hourly profit, in this case, is presented in Figure 5.3, the profit in red is a negative profit due to replenishing the energy of the two DBs received from the two customers arriving at the beginning of the day. Meanwhile, there are no EV arrivals at these time slots to achieve revenue from swapping. This operation resulted in a total daily profit of $2073.5, 150 customers were served, and 162 batteries were swapped.

5.3. Case Study III (Day-Ahead Scheduling with Perfect Forecasting)

In this case study, day-ahead scheduling is applied on the same actual EV arrival data in the unscheduled operation case impractically assuming that the swapping requests were perfectly forecasted in advance. Figure 5.4 Shows the SOC for a sample of three batteries during the day. The simulation starts with fully charged batteries. It can be seen that the customers arriving at the end of the day will not be served, since all batteries are charging to achieve SOC above 90% at the end of the day according to (5.1). The high energy consumed at the end of the day to charge all the depleted batteries before the next day resulted in a negative profit at the last two hours of the day as shown

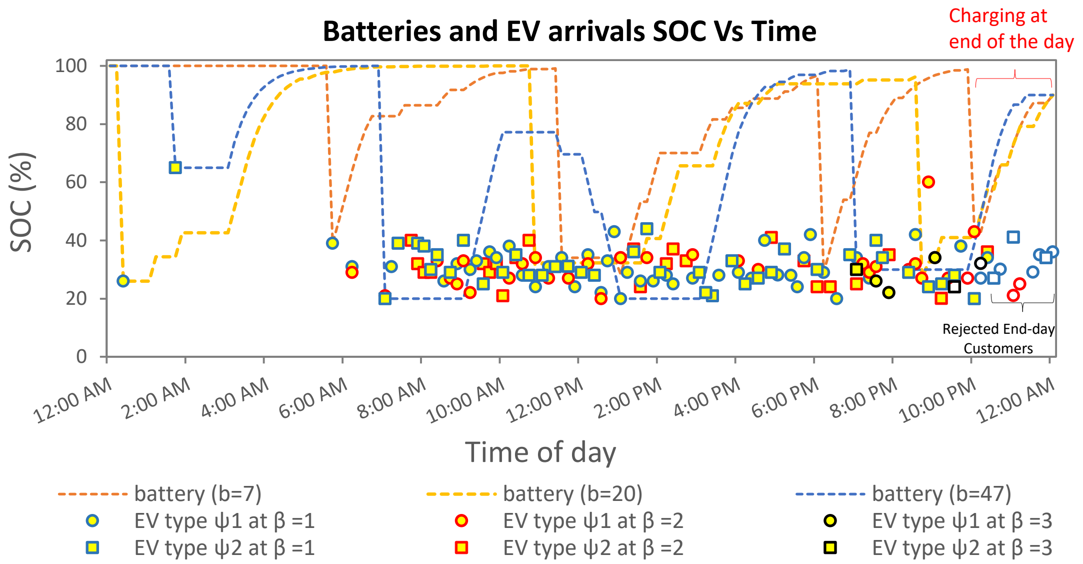

Figure 5.4. Day-ahead operation of the BSS

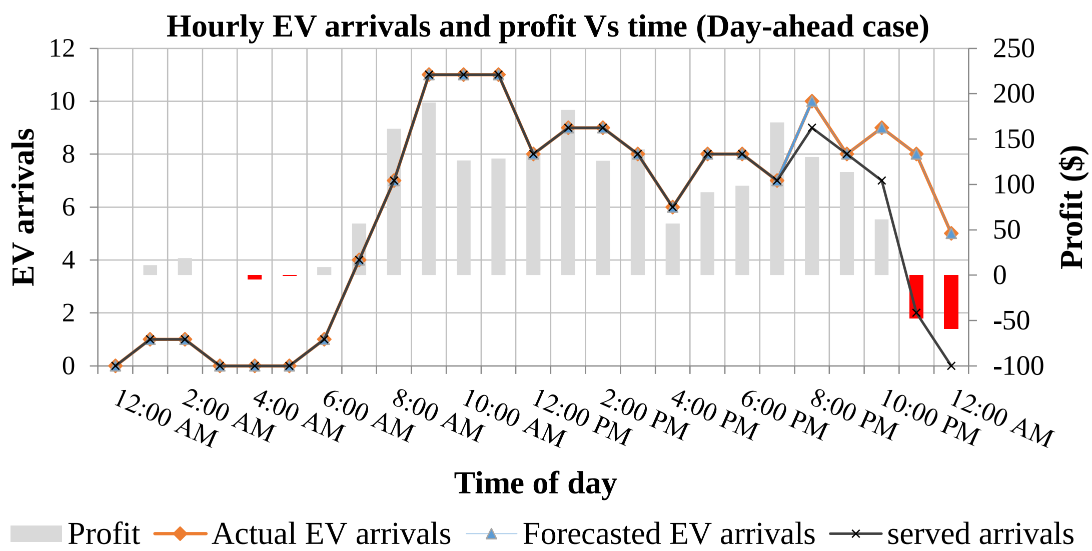

Figure 5.5: The profit and the number of EVs in the day-ahead operation case.

in figure 5.5. The day ahead scheduling resulted in a total daily profit of $1889.9 while serving 136 customers and swapping 142 battery units. However, day-ahead could achieve more profit by serving end-day customers if (5.1) is eliminated, in this case, it should be assumed that the BSS receives newly charged batteries at the beginning of the next day that was previously charged elsewhere. In Figure 5.6, the total B2G, G2B, and B2B power of the BSS at any time during the day is represented. It can also be observed that the optimization favored discharging to the grid at the highest grid price.

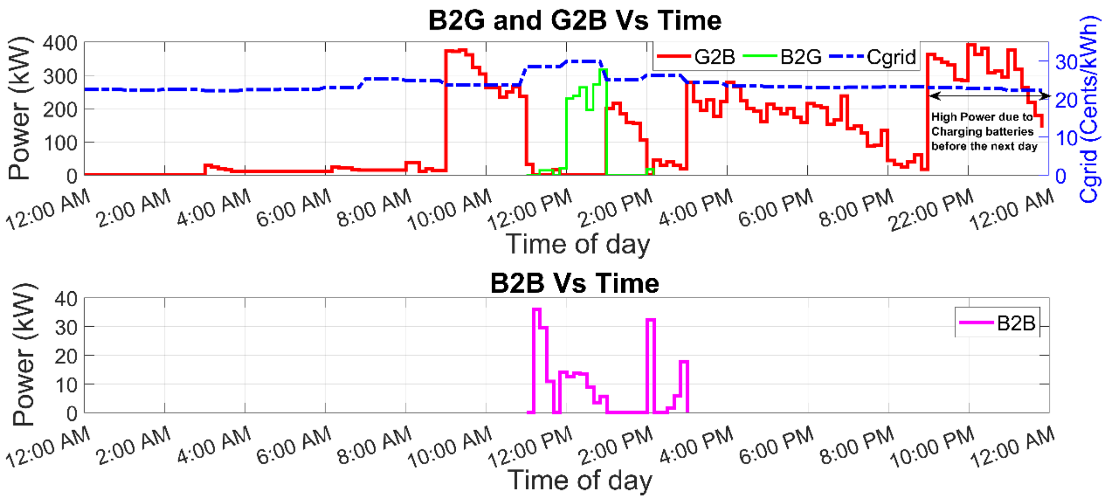

Figure 5.6: Total energy charged and discharged from the power grid and battery-to-battery energy exchange in day-ahead operation

5.4. Case Study IV (Rolling Horizon Scheduling)

This case study assesses the BSS dynamic scheduling using a rolling horizon optimization environment. The scheduling horizon is 24 hours of the day. The control horizon is the 10 minutes time slot, whereas a forecasting horizon of 6 hours is used. Forecasting is carried out for each battery type independently. In Figure 5.7, the LSTM network uses the historical data of four consecutive days of the EV arrivals requesting battery type ψ_1 to forecast future arrivals. The historical data of the EV arrivals were recorded every 10 minutes. The LSTM network state is continuously updated with the actual EV arrivals in the control horizon to update the forecasting horizon. For comparison, the actual EV arrivals data are the same data used in the unscheduled and day-ahead operation case studies.

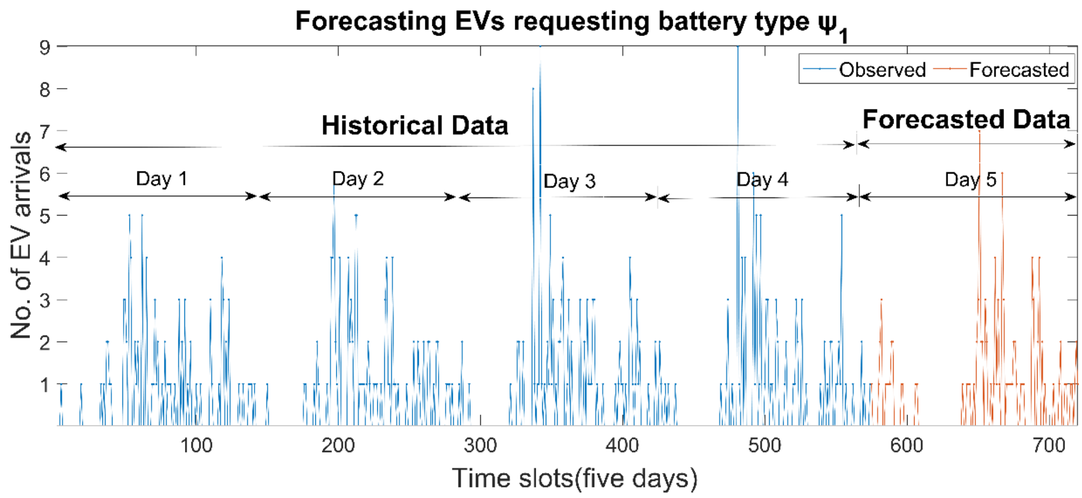

Figure 5.7. Forecasting for the arrivals of customers requesting a certain type of battery.

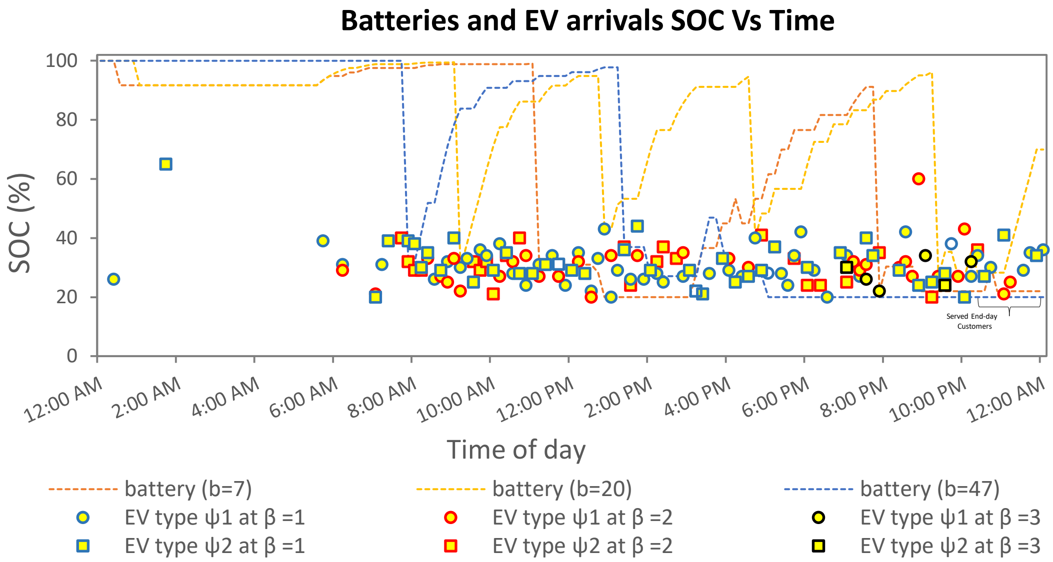

Figure 5.8. RHO scheduling of BSS.

One of the merits of the proposed RHO mechanism is that it runs continuously and it's not mandatory to have charged batteries at the end of the day. Unlike day-ahead operation, the RHO continues scheduling for the new day after the day ends while always ensuring the SOC of the charged batteries are above 90% before swapping according to (3.11) in section III, thus serving end-day customers as shown in Figure 5.8. The B2G discharge at the beginning of the day in Figure 5.10 took place since the 6 hours forecasting horizon initially contained a few arrivals so excess energy was available for discharging, however as the window rolls more customers appear in the

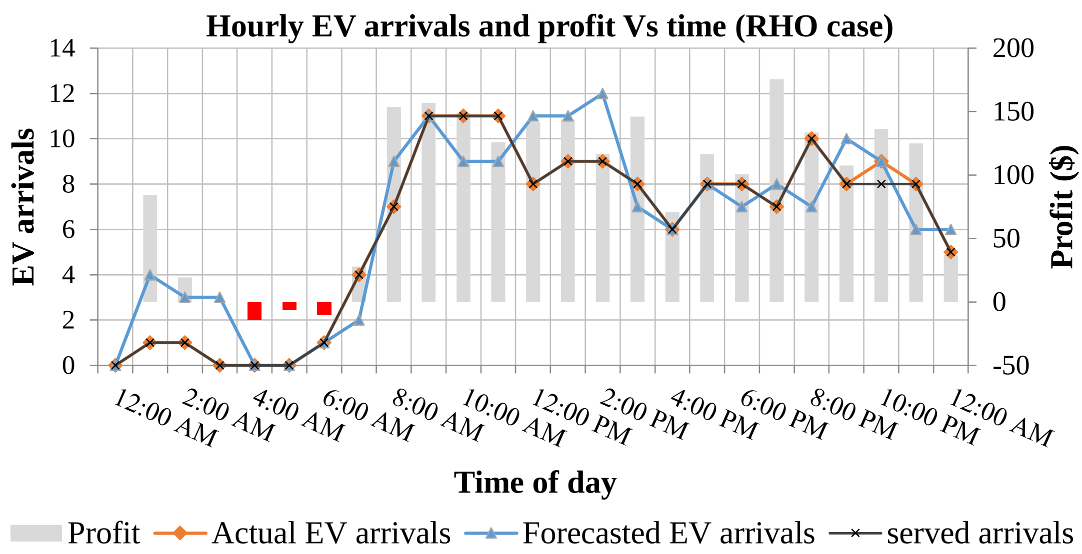

Figure 5.9: The profit and the EV arrivals in the RHO operation case study.

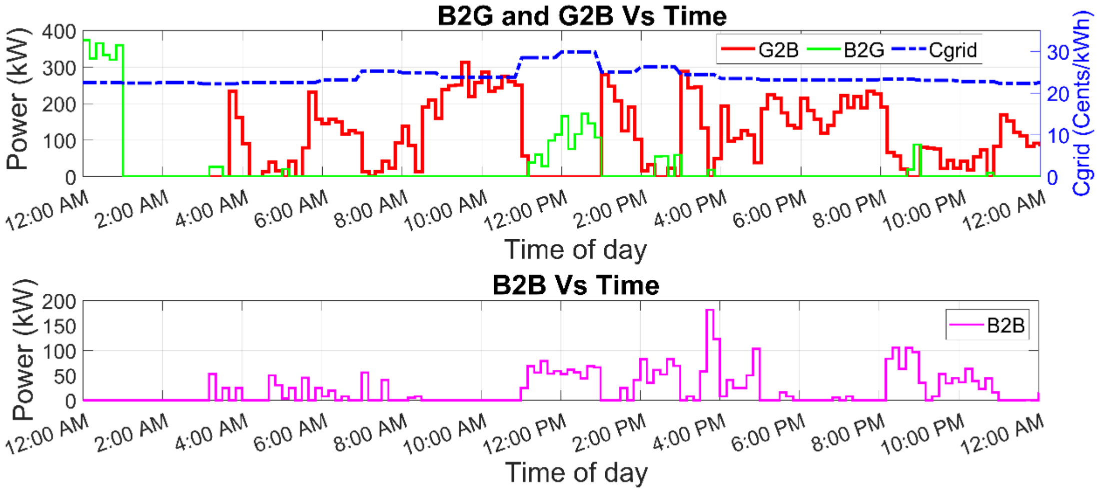

Figure 5.10: Total energy charged and discharged from the power grid & battery-to-battery energy exchange in RHO operation.

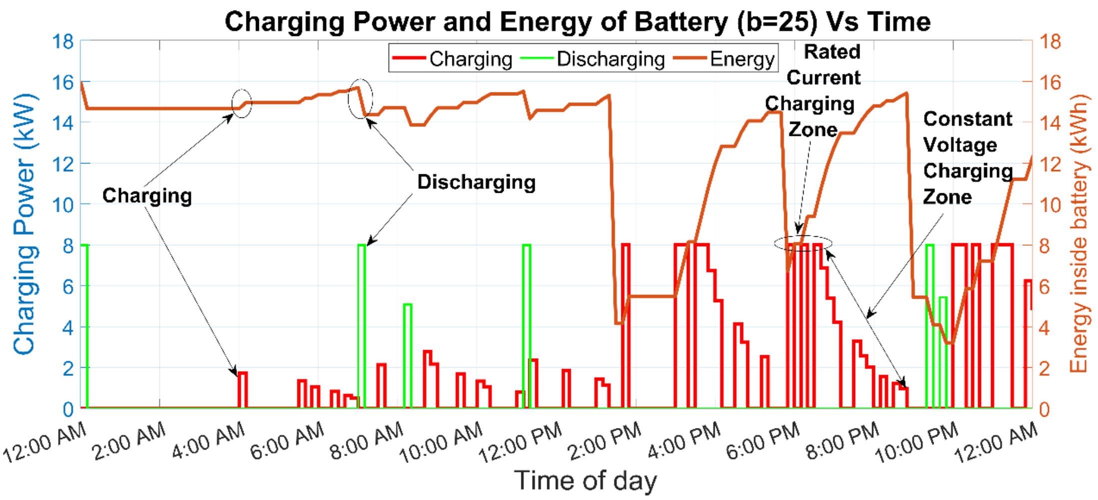

Figure 5.11. The charging power and energy are stored inside batteries indexed (b=25).

forecasting horizon and the batteries are charged in advance to serve the forecasted customers, this is also reflected in Figure 5.9 as a high profit at the beginning of the day then a negative profit for preparing the batteries after the customers showed up in the forecasting horizon. The RHO served 149 customers by swapping 158 battery units and resulted in a total daily profit of $2235.6 which is more than the previous cases. Although, the customers served, in this case, are nearly the same as the unscheduled operation but it's economically better due to discharging to the power grid. In Figure 5.11, the variable charger characteristics are presented, as it shows the energy and the charging power of a battery of type $\psi_1$with index (b = 25). It can be noticed that the charging rate has a kind of exponential decrease from the maximum charging rate in the constant voltage charging mode when the battery SOC exceeds (k = 70%).

Chapter 6 . BSS Planning

In this chapter, we employ an optimal planning strategy of BSS while incorporating PV generation to minimize the operational costs. The importance of this planning stage is to decide about the size of the BSS system and its resources. Due to the high cost of batteries, chargers, and the size of the BSS infrastructure in general, unreasonable planning will cost more investments and extra maintenances on fundamental equipment. Not only are we interested in the sizing of the BSS system and resources but also we are concerned about the optimal allocation of the BSS in the distribution systems. To provide adequate modeling for the system taking uncertainty into account probabilistic models are considered for modeling the PV generation output and the battery swapping demand.

6.1. System Costs

The traditional planning problems split the system costs into two main parts: the investment capital cost (CAPEX) and the operational costs (OPEX). OPEX includes mainly the cost of energy purchased from the grid, the cost of energy losses. CAPEX includes the cost of investment for the BSS resources (e.g. the number of batteries, the number of chargers, and the number of swapping bays). Traditional systems usually ignore the cost of maintenance and recycling and disposal costs. Hence, the maintenance and disposal costs are included in this research.

6.2. Modeling of PV

To model the PV module output power we utilize the historical data of the solar irradiance and the ambient temperature of the site as well as the characteristics of the module itself. The PV output power of the module is calculated as in (6.1)-(6.5). The historical PV output power and Markov Chain Monte Carlo (MCMC) simulation method are utilized to generate N_{scen}virtual scenarios of the PV power. Each year is clustered into 4 days, each day represents a season, each is denoted by $q \in \{1, 2, \cdots, 4\}$, The historical data of each season is used, such that each day d is divided into 24 hourly time segments $\tau \in \{1, 2, \cdots, 24\}$. It's assumed that the weather conditions for each time slot τ are the same for the whole q^{th} season. The PV output power historical data is clustered into Y states using the k-means algorithm except the first state is generated separately as it represents the lack of sunlight at night with a minimum output power of

Algorithm 2: Pseudo code for generating PV scenarios

Input: Matrix of PV output power historical data for each season $\mathbf{P}_{\boldsymbol{q}}^{\mathbf{hist}} \in \mathbb{R}^{N_q \times N_T}$.

Output: Matrix of PV output power virtual scenarios for $\mathbf{P}^{\boldsymbol{q}}$ of size $N_{scen} \times N_T$.

for $q = 1$ to N_{season} **do,**
  Cluster PV historical output data into [Y states]⟵k-means($\mathbf{P}_{\boldsymbol{q}}^{\mathbf{hist}}$, Y);
  Round the historical data to the nearest y^{th} state;
  Normalize the historical data to per unit values;
  Set the initial state at ($\tau = 1$) as ones vector $\mathbf{I}_{\boldsymbol{\tau}} = \mathbf{1}_{\boldsymbol{N_{scen}} \times \mathbf{1}}$;
  for $\tau = 1$ to 23 **do,**
    Build the transition matrix $\mathbf{G}_{\boldsymbol{q,\tau}}$ as in (6.6);
    Build the discrete cumulative transition matrix $\mathbf{G}_{\boldsymbol{q,\tau}}^{\mathbf{cdf}}$ as in (6.7);
    for $s = 1$ to N_{scen} **do,**
      Generate a uniformly distributed random variable u;
      $l = \mathbf{I}_{\boldsymbol{\tau}}(s)$;
      Apply discrete inverse CDF as in (6.8) and update [$o \leftarrow \mathrm{DICDF}(u)$];
      $\mathbf{I}_{\boldsymbol{\tau+1}}(s) = o$;
      Map the o^{th} state to its corresponding PV output power value;
      Store the mapped state PV-power in $\mathbf{P}^{\boldsymbol{q}}(s, \tau + 1)$;
    end for
  end for
end for
return;

$$T_{cell} = T_A + S_{IR} \times \left(\frac{\mathrm{NOCT} - 20}{0.8\ \mathrm{kW/m^2}}\right) \tag{6.1}$$

$$I_{pv} = S_{IR} \times \left(I_{sc} + \mathrm{KI}(T_{cell} - 25)\right) \tag{6.2}$$

$$V_{pv} = V_{oc} - \mathrm{KV}(T_{cell} - 25) \tag{6.3}$$

$$\mathrm{P^{pv}} = N_{cells} \times FF \times V_{pv} \times I_{pv} \tag{6.4}$$

$$FF = \frac{V_{MPP} \times I_{MPP}}{V_{oc} \times I_{sc}} \tag{6.5}$$

0 p.u for the PV system, for the rest of the states each range of PV output is grouped into one state. The generation of N_{scen} annual scenarios are detailed in Algorithm 2. The algorithm is initialized and starts building a transition matrix $\mathbf{G}_{\boldsymbol{q},\boldsymbol{\tau}}$ for every hour τ of the day. The transition matrix represents the probability of transition from all states at time τ to all states $\tau + 1$. Since the transition matrix is calculated for each time slot the total number of transition matrices for all seasons is $24 \times 4 = 96$ matrices. Each element in the transition matrix $g_{l,o}$ shows the probability of occurrence of state o at time $\tau + 1$ if the previous state was l at time τ. The transition matrix elements can be obtained as follows:

$$g_{lo} = P(y_\tau = o \,|y_{t+1} = l) = \frac{n_{lo}}{\sum_y n_{ly}} \qquad \forall l, o \in \{1, 2, \cdots, \mathrm{Y}+1\}, \tag{6.6}$$

where n_{lo} is the number of transitions from state l at τ to state o at $\tau + 1$. After obtaining all the transition matrices the discrete transition CDF matrices $\mathbf{G}_{\boldsymbol{q},\boldsymbol{\tau}}^{\mathbf{cdf}}$ are constructed as in (6.7)

$$g_{lo}^{cdf} = \sum_{1}^{o-1} P(y_\tau = o \,|y_{\tau+1} = l) \qquad \forall l \in \{1, 2, \cdots, \mathrm{Y}+1\}, \tag{6.7}$$

where g_{lo}^{cdf} represent the elements of the discrete CDF matrix. The CDF matrix can be then used to generate N_{scen} scenarios using the Discrete Inverse CDF (DICDF) method as in (6.8)

$$CDF^{-1}(u) = \mathbf{inf}\{\, o : \left[g_{l1}^{cdf}, g_{l2}^{cdf}, \cdots, g_{lo}^{cdf}\right] \geq u\} \qquad \forall l \in \{1, 2, \cdots, \mathrm{Y}+1\}, \tag{6.8}$$

where u is a uniformly distributed random variable.

The scenario generation algorithm is applied to generate 1000 scenarios for each season. A sample of the generated scenarios for each season is presented in Figure 6.1. To speed up optimization problems generated virtual scenarios are usually reduced using one of many scenario reduction techniques while taking the weight of each scenario as a representation for the probability of its occurrence.

Algorithm 3: Virtual scenario reduction using k-means

Input: Matrix **X** with N_{scen} virtual scenarios and dimension N_T; **X** $\in \mathbb{R}^{N_{scen}\times N_T}$

Output: A matrix **R** of K_m centroids reducing the scenarios; **R** $\in \mathbb{R}^{K_m\times N_T}$,

A Vector that has the probability of each centroid (reduced scenario) **W** $\in \mathbb{R}^{K_m\times 1}$

Initialize A vector of cluster indices assigned to each scenario **C** $\in \mathbb{R}^{N_{scen}\times 1}$

//***Multiple random initializations***

for $r = 1\ to\ N$

Initialize $\mathrm{K_m}$ cluster centroids and store in $\boldsymbol{\mu}^r = \{\mu_1, \mu_2, \cdots, \mu_k\}$; where $\mu_k \in \mathbb{R}^{1\times N_T}$

for $s = 1$ to N_{scen} **do**,

$\mathrm{J}^{(\mathrm{r})} = \sum_k \sum_s \left\| x^{(s)} - \mu_k \right\|^2$;

end for

end for

Select best $\mathrm{K_m}$ initial centroids corresponding to r^{th} initialization $r \leftarrow \mathrm{argmin}\left(\mathrm{J}^{(\mathrm{r})}\right)$

Save the best initial centroids $\boldsymbol{\mu}^{\boldsymbol{r}}$

repeat{

//***Cluster assignment***

for $s = 1$ to N_{scen} **do**,

$\mathbf{C}^{(s)} \coloneqq \underset{\mu_k}{\mathrm{argmin}} \left\| x^{(s)} - \mu_k \right\|^2$

end for

//***Move centroid***

for $k = 1$ to $\mathrm{K_m}$ **do**,

$\mu_k \coloneqq \frac{1}{|c_k|} \sum_{s\in c_k} x^{(s)}$

end for

until the centroid position don't change**}**

$\mathbf{W}^{(k)} = \frac{\sum_k \mathbf{C}^{(k)}}{N_{scen}}, \forall k \in K_m$

return R $\leftarrow [\mu_1, \mu_2, \cdots, \mu_k]^{\mathbf{T}}$, **W**

The generated N_{scen} scenarios can be further reduced into $\mathrm{K_m}$ scenarios using k-means algorithm for this purpose as detailed in Algorithm 3. In Algorithm 3 the used k-means algorithm starts by initializing the centroids with r multiple random initializations of $\mathrm{K_m}$ centroids, each centroid μ_k is N_T dimensional vector; where $N_T =$ 24 time slots. Hence, the best initial centroid is selected using multiple random initializations and k- means algorithm is performed over two well-known steps-namely: the cluster assignment step and the moving of the centroid step. Finally, the centroids reducing the N_{scen}virtual scenarios are saved and the probability of each is calculated as detailed in Algorithm 3. Figure 6.2 shows the results of the scenario reduction algorithm to reduce the 1000 PV scenarios generated for the spring season to only five scenarios.

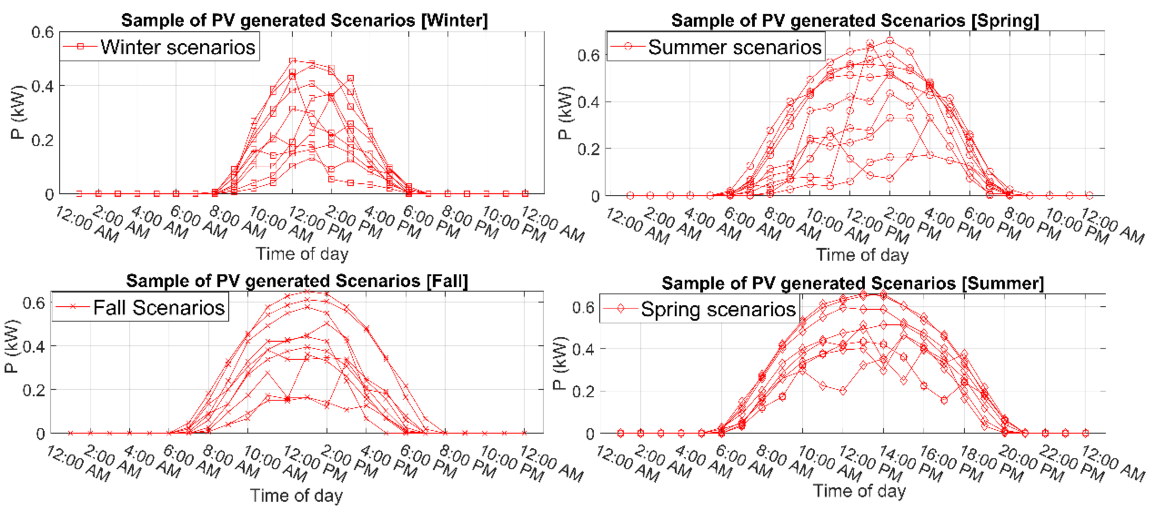

Figure 6.1: A sample of the generated PV scenarios for each season

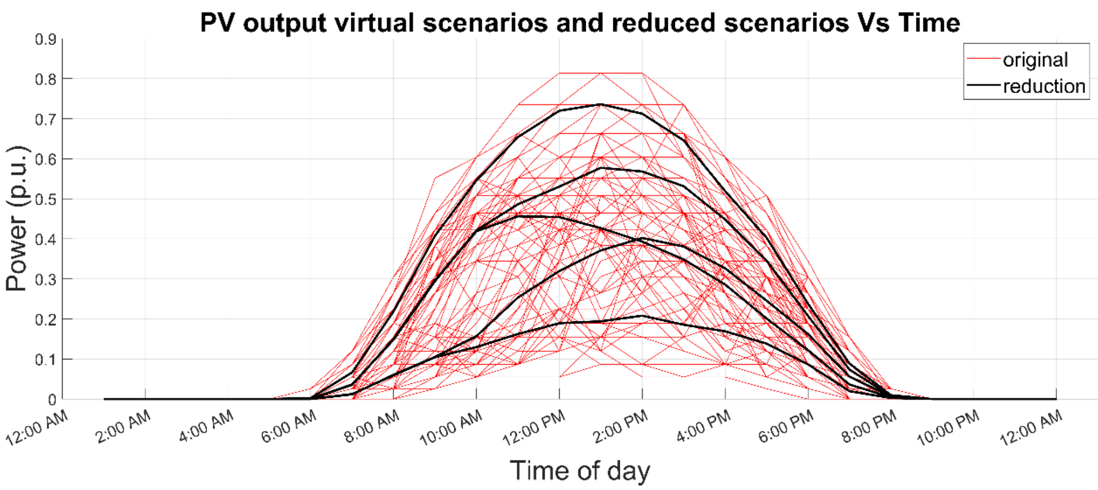

Figure 6.2: Scenario reduction for the generated scenarios of PV output power in the spring season

6.3. Modeling of EV Arrival Rates

A generalized model utilizing the Monte Carlo simulation (MCS) technique is proposed for probabilistic modeling of EV arrivals. The EV arrivals historical data is used is obtained from several EV charging stations in Toronto, Ontario, Canada. The proposed EV arrivals model is detailed in the flow chart in Figure 6.3. As clarified in the figure, the historical hourly data of EV arrivals are clustered into 4 seasons each season is divided into weekday and weekend. Hence, the entire year is modeled as 8 days; 2 days for each season. Each day has 24 hourly time slots.

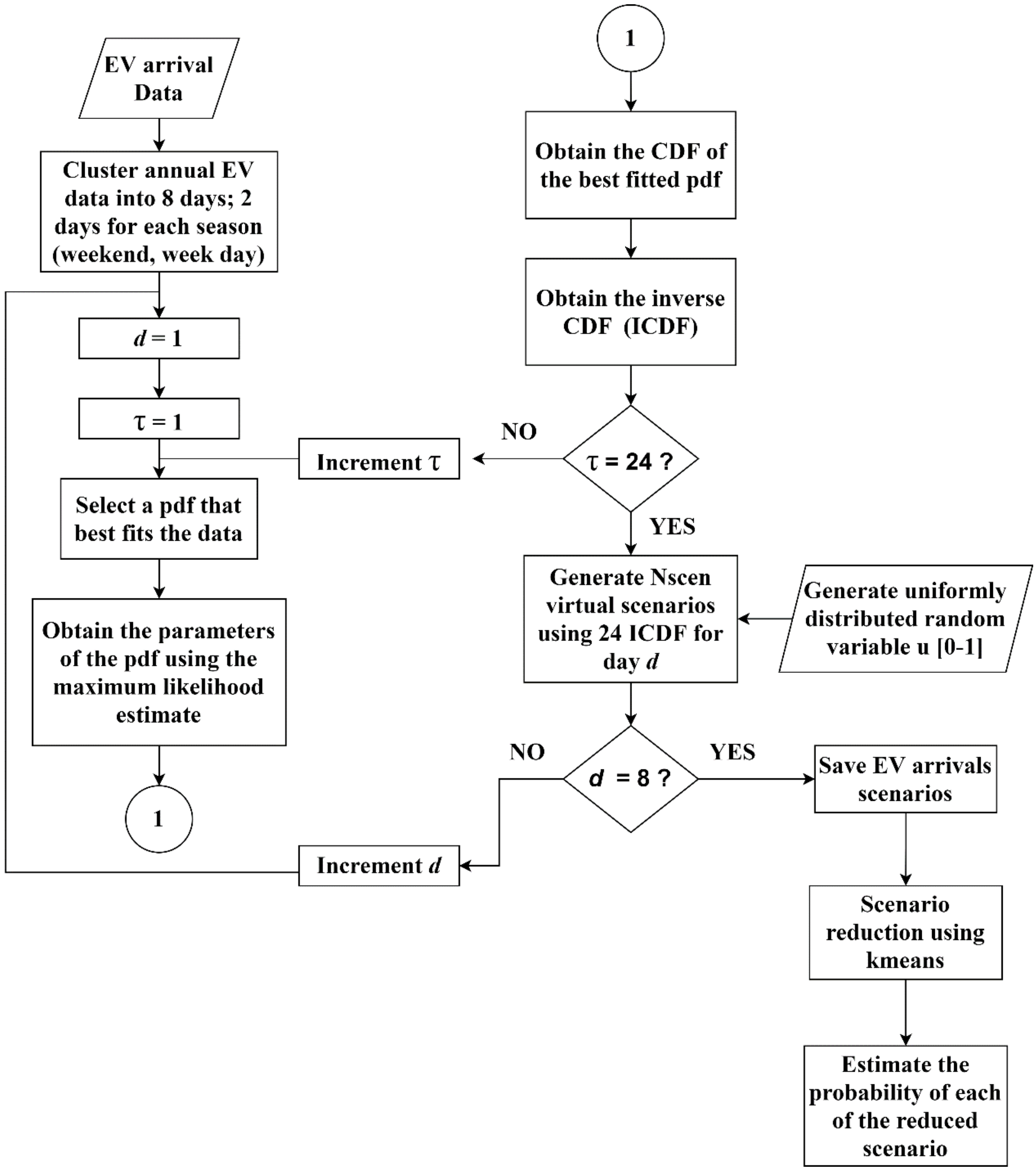

Figure 6.3: The proposed EV arrival rate scenario generation model

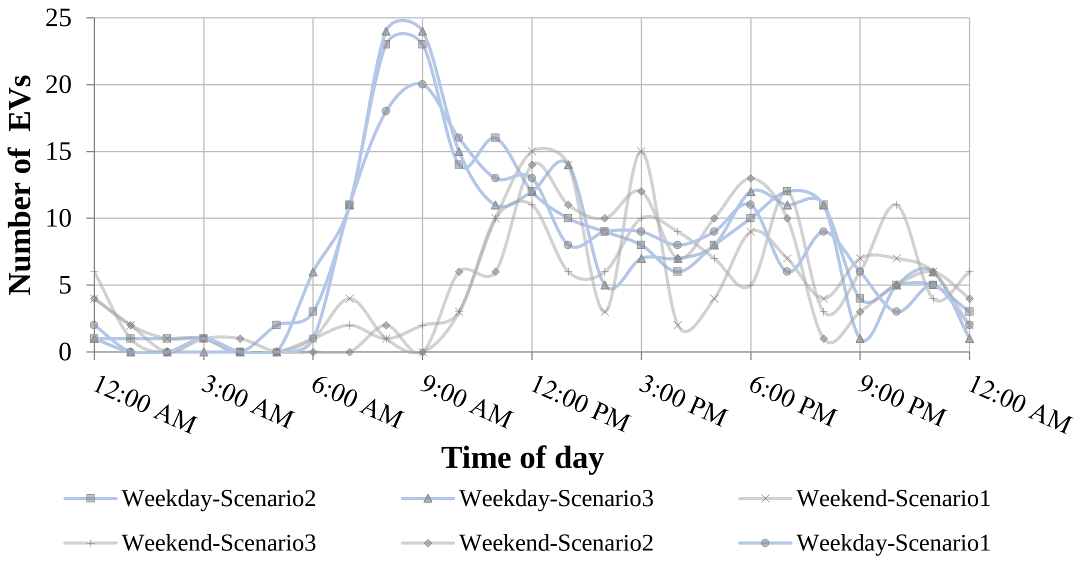

Figure 6.4: Sample of the generated scenarios of EV arrivals for weekend and week day in the spring season.

The Maximum likelihood estimate is used to fit the hourly historical data of each of the eight days using different PDFs for each hour. The CDF for each hour of the eight days is obtained and denoted by $V_{d,\tau}$. The EV arrivals virtual scenarios for each day d are generated using the well-known inverse CDF method and stored in the matrix $\mathbf{E}_{\boldsymbol{d}} \in \mathbb{R}^{N_{scen} \times N_T}$, each element in the d^{th} matrix is $e_{d,s,\tau}$ as shown in (6.9).

$$e_{d,s,\tau} = \mathrm{ICDF}_{V_{d,\tau}}(u_s) \qquad \forall d, s, \tau \leq N_{scen} \tag{6.9}$$

The generated EV arrivals scenarios are reduced by k-means clustering as explained earlier in Algorithm 3. Moreover, a sample of 6 virtual scenarios for the EV hourly arrival rate in the spring season is presented in Figure 6.4. As shown in the figure, the weekday and weekend are represented by 3 scenarios each.

6.4. Optimization Problem Formulation

This section describes the mathematical formulation of the PV-based BSS planning problem while incorporating the BSS allocation in the distribution network. The problem is formulated as a mixed-integer linear programming (MILP) and is based on the following fitness function.

6.4.1. The objective function. The objective function used for the BSS planning problem is mainly to maximize the annualized profit as follows

$$\max_{Z,\rho_1,\rho_2} = AR - ACO - ACI - AS - ACM \tag{6.10}$$

where Z is the decision variable vector including the operational decision variables as illustrated in chapter 3 in addition to the newly added decision variable related to charging from the PV system $Z = \left(p_{\tau,b}^{ch}, p_{\tau,b}^{dch}, ch_{\tau,b}, sw_{\tau,b,\beta}, p_{\tau,b}^{chpv}\right)^T$. ρ_1 and ρ_2 are the sets of the decision variables representing the BSS installed resources and location in the distribution network respectively. Such that the set $\rho_1 = \{N^{bat}, N^{ch}\}$ includes the number of batteries and chargers which are considered as the main assets for the BSS system and $\rho_2 = \{i\}$ where i is the index of the bus in the distribution system to which the BSS is connected to. For suitable economic analysis, the CAPEX is represented by equal annual payments over the project life cycle l_c, using the capital recovery factor (CRF), whereas the OPEX is also annualized and levelized using the levelization factor (LF), thus we have

$$\text{CRF} = \frac{d(1+d)^{l_c}}{(1+d)^{l_c} - 1} \tag{6.11}$$

$$\text{LF} = \text{CRF} \times \frac{(1+d')^{l_c} - 1}{d'(1+d')^{l_c}}, \quad d' = \frac{d-e}{1+e} \tag{6.12}$$

where d is the discount rate; d' is the effective discount rate; e is the escalation factor.

Due to the increase in the fuel prices which would consequently increase the prices of electricity during the project life cycle, As result, the annual cost of operation(ACO), the annual salaries of the employees(AS), and the annual revenue (AR) are to be levelized.

The probability of each of the PV and the EV arrivals reduced scenarios $\mathrm{K_m}$ are permutated together to have a total number of reduced scenarios [$\mathrm{K_m}$ PV scenarios × $\mathrm{K_m}$ EV arrivals scenarios]. The AR determines the revenue generated from the BSS operations by swapping and discharging energy to grid. The AR is levelized due to the escalation in the service price with the number of years as follows:

$$AR = \text{LF} \times \sum_{d=1}^{8} N_d \sum_{k=1}^{\mathrm{K_m}} w_d{}^{(k)} \left[R^s + R^{B2G} + R^{PV2G}\right]_{d,k} \tag{6.13}$$

$$R^{PV2G} = \sum_{(\tau \in Tpv)} \left(\mathrm{P}_{\tau}^{\mathrm{pv}} \times \mathrm{c}_{\tau}^{\mathrm{gr}} - \sum_{(b \in B)} p_{\tau,b}^{chpv} \times \mathrm{C}^{\mathrm{pv}} \right) \Delta \mathrm{t} \tag{6.14}$$

where R^s and R^{B2G} are demonstrated already in chapter 3; R^{PV2G} is the revenue from discharging excess PV generation to the power grid; ${w_d}^{(k)}$ is the weight of the k^{th} scenario in the d^{th} day; N_d is the number of days represented by a particular day d.

The annualized cost of operation(ACO) can be calculated by:

$$ACO = \mathrm{LF} \times \sum_{d=1}^{8} N_d \sum_{k=1}^{K_m} {w_d}^{(k)} \left[C^{G2B} + \mathrm{CE}^{\mathrm{loss}}\right]_{d,k} \tag{6.15}$$

$$\mathrm{CE}^{\mathrm{loss}} = \sum_{\tau \in T} P_{\tau}^{loss} \times \Delta \mathrm{t} \times C_{loss}^{kWh} \tag{6.16}$$

The annualized cost of investment (ACI) can be calculated by:

$$ACI = \mathrm{CRF} \times [C_{batt} + C_{ch}] \tag{6.17}$$

$$C_{batt} = N^{bat} \times \mathrm{Pr}^{\mathrm{bat}} \tag{6.18}$$

$$C_{ch} = N^{ch} \times \mathrm{Pr}^{\mathrm{ch}} \tag{6.19}$$

where C_{batt} and C_{ch} are the investment costs of batteries and chargers at the BSS respectively; $\mathrm{Pr}^{\mathrm{bat}}$ and $\mathrm{Pr}^{\mathrm{bat}}$ are the prices per battery unit and charger respectively.

The annualized salaries of the employees and the cost of maintenance are levelized using the following equations:

$$AS = \mathrm{LF} \times \text{Total annual salaries of employees} \tag{6.20}$$

$$ACM = \mathrm{LF} \times \text{Total annual cost of maintenance} \tag{6.21}$$

6.4.2. Operation constraints of the PV-based BSS system. The BSS operational constraints used for the planning problem are slightly modified from those used in chapter 3 to incorporate the PV system. At this point, it is also assumed that the BSS operations are considering only a specific type of battery and charger. The BSS problem is subjected to the following constraints:

Constraints (3.6), (3.10)-(3.12), (3.18), (3.20), (3.21), (24-28) in chapter 3, and

$$soc_{\tau,b} = soc_{\tau-1,b} + \frac{\left(p_{\tau,b}^{ch} + p_{\tau,b}^{chpv} - p_{\tau,b}^{dch}\right) \times \Delta t}{\mathrm{e}_b^{\max}} \times 100 - \Delta soc_{\tau,b}^{swap} \tag{6.22}$$

$$\forall(\tau \geq 2) \in T, \forall\, b \in B,$$

$$soc_{\tau,b} = \mathrm{soc}_b^0 + \frac{\left(p_{\tau,b}^{ch} + p_{\tau,b}^{chpv} - p_{\tau,b}^{dch}\right) \times \Delta t}{\mathrm{e}_b^{\max}} \times 100 - \Delta soc_{\tau,b}^{swap} \tag{6.23}$$

$$(\tau = 1) \in T, \forall\, b \in B,$$

$$0 \leq p_{\tau,b}^{ch} + p_{\tau,b}^{chpv} \leq \mathrm{P}^{\mathrm{MAXc}} \times ch_{\tau,b} \qquad \forall \tau \in T, b \in B, \tag{6.24}$$

$$p_{\tau,b}^{chpv} = 0 \qquad \forall \tau \in Tpv', b \in B,$$

$$0 \leq p_{\tau,b}^{dch} \leq \mathrm{P}^{\mathrm{MAXd}} \times dch_{\tau,b} \qquad \forall \tau \in T, b \in B, \tag{6.25}$$

$$ch_{\tau,b} + dch_{\tau,b} + \sum_{(\beta \in U)} sw_{\tau,b,\beta} \leq 1 \qquad \forall \tau \in T, \forall\, b \in B, \tag{6.26}$$

$$\sum_{(b \in B)} p_{\tau,b}^{chpv} \leq \mathrm{P}_\tau^{\mathrm{pv}} \tag{6.27}$$

$$\forall \tau \in T,$$

$$\mathrm{P}_\tau^{\mathrm{pv}} - \sum_{(b \in B)} p_{\tau,b}^{chpv} + \sum_{(b \in B)} p_{\tau,b}^{dch} \leq \mathrm{p}^{\mathrm{GRIDd}} \tag{6.28}$$

$$\forall \tau \in T,$$

The total BSS power exchange with the power grid can be calculated as in (6.29), where the term P_τ^{BSS} is positive when the BSS is discharging to the power grid and it's negative when the BSS is charging from the power grid. The total BSS power exchange with the grid is treated as a distributed energy storage connected to one of the distribution system buses as elaborated in the following section.

$$P_\tau^{BSS} = \left(\mathrm{P}_\tau^{\mathrm{pv}} - \sum_{(b \in B)} p_{\tau,b}^{chpv}\right) + \sum_{(b \in B)} p_{\tau,b}^{dch} - \sum_{(b \in B)} p_{\tau,b}^{ch} \tag{6.29}$$

$$\forall \tau \in T.$$

6.4.3. Operation constraints of the distribution system. The objective function in (6.10) is subjected to the constraints of the active and reactive power flow equations for each bus i and at all the time slots of the day τ as in (6.30) and (6.31)

$$P_{i,\tau}^{grid} + P_{i,\tau}^{BSS} - \mathrm{P}_i^{\mathrm{D}} \times \mathrm{R}_\tau = \sum_{j \in \mathcal{B}} V_{i,\tau} V_{j,\tau} \mathrm{Y}_{i,j} \cos\left(\gamma_{i,j} + \delta_{j,\tau} - \delta_{i,\tau}\right) \tag{6.30}$$

$$\forall i \in \mathcal{B} \;\; \forall \tau \in T,$$

$$Q_{i,\tau}^{grid} - \mathrm{Q}_i^{\mathrm{D}} \times \mathrm{R}_\tau = -\sum_{j\in\mathcal{B}} V_{i,\tau} V_{j,k} \mathrm{Y}_{i,j} \sin(\gamma_{i,j} + \delta_{j,\tau} - \delta_{i,\tau}) \quad \forall i \in \mathcal{B} \;\; \forall \tau \in T, \tag{6.31}$$

The main substation in the distribution system is connected to bus $i = 1$, such that the injected active and reactive power are represented by equations (6.32)-(6.34)

$$P_{i,\tau}^{grid} = 0 \quad \forall i \neq 1, \forall \tau \in T, \tag{6.32}$$

$$0 \leq P_{i,\tau}^{grid} \leq \mathrm{P}_{\max}^{\mathrm{grid}} \quad \forall i \in \mathcal{B} \;\; \forall \tau \in T. \tag{6.33}$$

$$0 \leq Q_{i,\tau}^{grid} \leq \mathrm{Q}_{\max}^{\mathrm{grid}} \quad \forall i \in \mathcal{B} \;\; \forall \tau \in T. \tag{6.34}$$

The bus voltage has to be kept within its minimum and maximum limits prescribed in the voltage regulation standards e.g. ANSI C84.1.

$$\mathrm{V}^{\max} \leq V_{i,\tau} \leq \mathrm{V}^{\min} \quad \forall i \in \mathcal{B} \;\; \forall \tau \in T. \tag{6.35}$$

The power loss in the system at any time τ is defined in (6.36). The power losses in the distribution network would be highly affected by the BSS location. Hence, The BSS allocation is an important key role to provide planning for these types of stations.

$$P_\tau^{loss} = \sum_{i\in\mathcal{B}} P_{i,\tau}^{grid} + P_{i,\tau}^{BSS} - \mathrm{P}_i^{\mathrm{D}} \times \mathrm{R}_\tau \quad \forall \tau \in T, \tag{6.36}$$

6.5. Proposed Solution

As mentioned earlier, the proposed formulation is a MILP problem. The problem is broken down into two interdependent sub-problems, namely-outer sub-problem and inner sub-problem each sub-problem separately is a MILP. The problem is solved using a combination of metaheuristic and deterministic approaches to managing the outer and inner sub-problems at the same time. A detailed flow chart is presented in figure 6.5 explaining the proposed solution mechanism. As shown in the figure, the genetic algorithm toolbox GA is implemented in the MATLAB environment as a metaheuristic technique for the outer search sub-problem, such that it aims to generate a set of candidate solution for the size of the installed assets ρ_1 and the location of the BSS in the distribution network ρ_2.

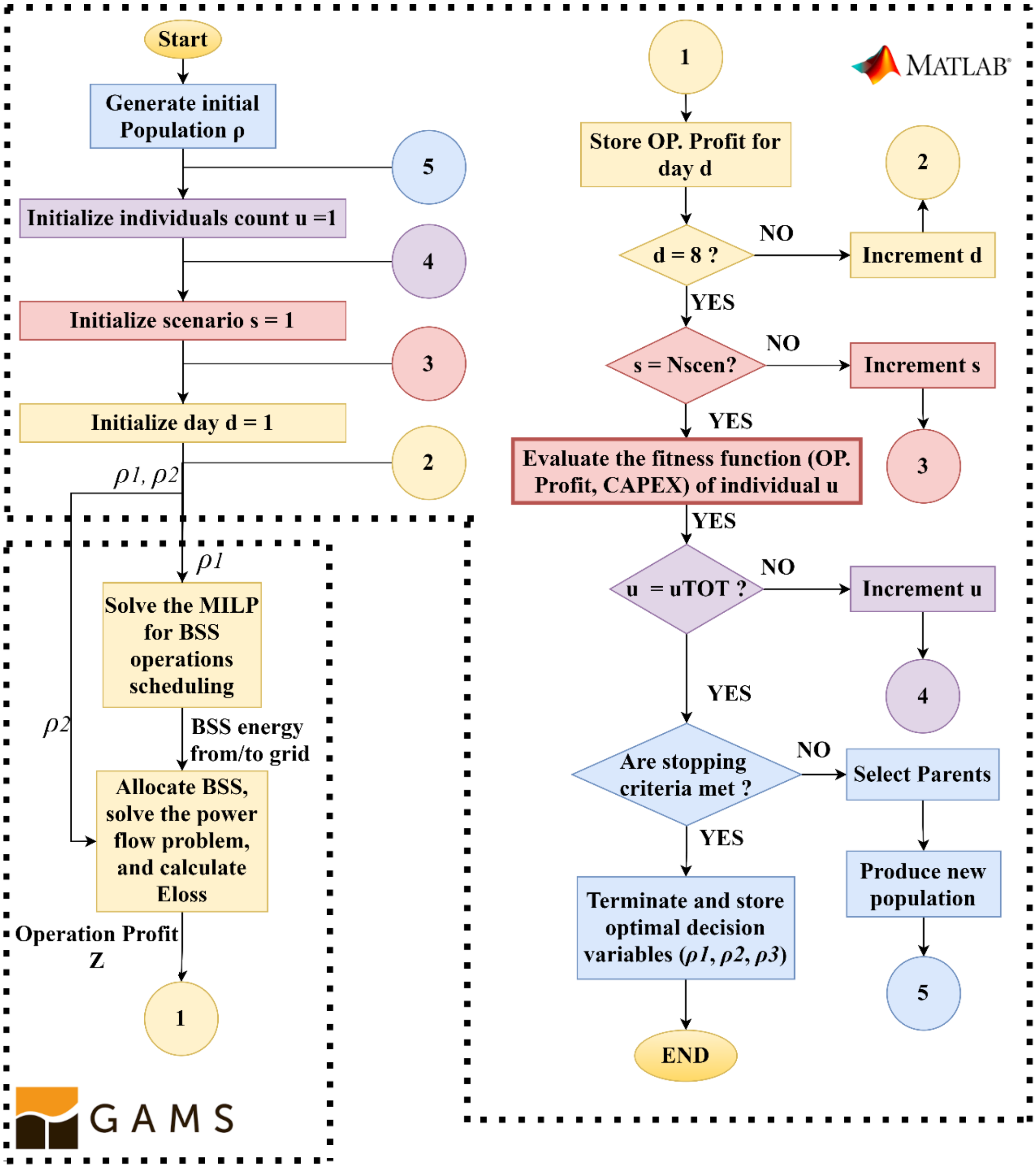

Figure 6.5: Proposed solution approach

As for the inner sub-problem, it mainly deals with the BSS operation scheduling as it handles the daily operational profit which is the difference between the daily operational revenue and the daily operational costs which is related to the annualized profit part in the objective $[AR - ACO]$. The inner sub-problem takes the variables ρ_1 and ρ_2 as inputs from the outer sub-problem and the solution of the problem yields to the set of decision variables z for the operation schedule. The inner problem is solved under the GAMS optimization environment as a day-ahead problem using the CPLEX MILP solver, such that the problem is solved for each day d for all the possible scenarios s. The main objective is to maximize the annualized benefits. Therefore, the outer problem receives the output from the inner problem which is $\left([R^{s} + R^{B2G} + R^{PV2G}]_{d,s} - \left[C^{G2B} + \mathrm{CE}^{\mathrm{loss}}\right]_{d,k}\right)$ for each day and scenario. Hence, each scenario s is multiplied by the probability of its occurrence ($w_{d}{}^{(k)}$) and each day d is multiplied by the frequency of its occurrence (N_{d}) and uses it in the fitness function of the GA until an optimal solution that maximizes the annualized profits is achieved.

6.6. Planning Results and Analysis

This section carries out the results of the BSS planning case study. The proposed planning framework is tested on the IEEE 38-bus distribution system shown in Figure 6.5. The system contains different types of loads: Industrial loads, commercial loads, and residential loads. The rated voltage of the system is 12.66 kV.

Table 6.1: Data of the BSS

Parameters	**Value**
Battery capacity	42 kWh
Swapped energy cost	0.5 $/kWh
Cost of labor, maintenance, and material	$3500/charger
Cost of the battery unit	4000 $
Cost of battery charger	5000 $
Cost of PV system	1400 $/kW
Capital Investment of BSS	3.5 MVAR
$\mathrm{DOD}^{\mathrm{max}}$	80%
Fixed swapping cost	12 $
$\mathrm{P}^{\mathrm{MAXc}}$, $\mathrm{P}^{\mathrm{MAXd}}$	25 kW
soc_{b}^{0}	100 %
ζ	90 %
$\Delta\mathrm{t}$	1/6
η^{ch}, η^{dch}	0.94

The total real and reactive load are equal to 3.715 MW and 2.3 MVAR respectively. The data of the system are given in [36]. The interest rate is assumed to be 6% and the escalation rate is assumed to be 2%. The parameters of the PV-based BSS are presented in Table 6.1. The BSS system is treated as if it's a large distributed energy storage (DES) system to be installed at one of the buses in the distribution system.

It's worth noting that in distribution network planning problems the candidate buses to install DES or DGs are usually selected based on a techno-economic planning analysis; however, it's out of the scope of this research work and assumed as inputs to this study. Hence, In this case study, we chose arbitrary ten candidate buses for installing the BSS, which are buses 28-38. The chosen candidate buses are distributed all over the test system to cover different regions as presented in figure 6.6. The table displays the operational parameters of the BSS and the installation prices for the planning purpose. Table 6.2 demonstrates the results obtained considering three cases: (a) BSS planning without allocation, (b) BSS planning with allocation, and (c) the distribution system Energy losses without BSS. After solving the planning problem the optimal planning chose the number of batteries at the BSS inventory to be 50 batteries and the number of chargers to be 38 chargers. Meanwhile, the optimal location for installing the BSS system is bus number $i = 36$. The optimal planning resulted in a total annualized profit of \$321,490/ year.

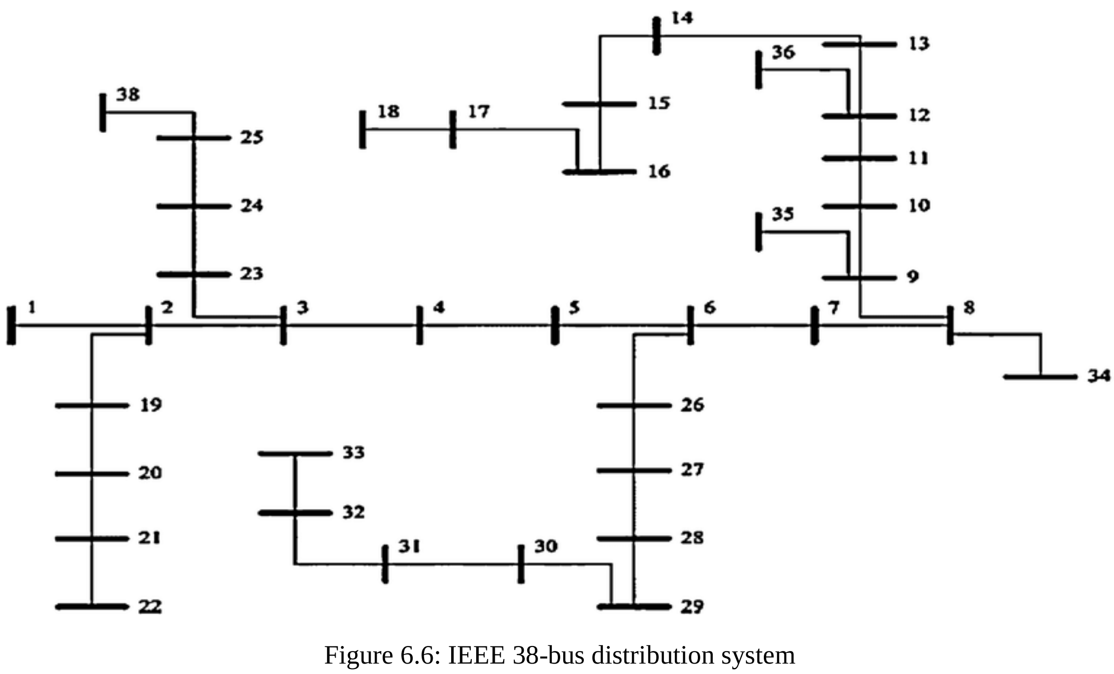

Figure 6.6: IEEE 38-bus distribution system

Table 6.2: Planning results

	BSS at bus $i = 30$	**BSS Allocation**	**Without BSS**
No. of batteries	45	50	
No. of chargers	45	38	
BSS optimal location		36	
Annualized profit (S)	315,910	321,490	
Annual Distribution system losses (MWh)	1312.5	1360.3	1249.61

Chapter 7 . Conclusion

Battery Swapping Stations (BSS) provides a fast alternative service compared to charging EVs at the charging stations. In this thesis, a new model for the dynamic operation of the BSS is presented in the operational phase. The goal of the model is to provide optimal dynamic scheduling of the batteries at the BSS for swapping and charging coordination using an LSTM-based (RHO) mechanism. The batteries at the BSS are scheduled to operate in B2G, G2B, and B2B modes. Battery heterogeneity and the diversity of the EV types are adopted in this model. Hence, the battery management is unified which achieved global gains. Furthermore, detailed modeling of the variable charger characteristics for charging lithium-ion batteries is provided instead of traditional constant current chargers to fully utilize the grid services. The optimization of BSS is modeled as Mixed-integer linear programming (MILP) and solved using an exact optimization approach to obtain an optimal solution that maximizes the total daily profit. Compared with unscheduled and day-ahead operations the dynamic RHO model of the BSS is more reliable and achieved higher profits. In the planning phase, an optimal planning approach is proposed to determine the size of the assets of the BSS system and to optimally allocate the BSS in the distribution system considering its impact on the distribution network. Moreover, the Markov Chain Monte Carlo (MCMC) simulation technique is utilized to tackle the uncertainty with the photovoltaic generation and the EV arrivals. The planning problem is broken into two interdependent subproblems and solved using a combination of metaheuristic and deterministic approaches to managing the two subproblems concurrently. Simulation results showed the effectiveness of BSS planning and an optimal solution is obtained which maximizes the annualized benefits. As a result, this thesis provides future guidance for BSS operators.

References

[1] Edison Electric Institute, "EEI celebrates 1 Million Electric Vehicles on U.S. Roads," November, 2018 [online]. Available: https://www.eei.org/resourcesandmedia/newsroom. [Accessed: May 1, 2021].

[2] What are the challenges facing electric vehicle adoption [online]. Available:https://www.sgfleet.com/global/news/what-are-the-challenges-facing-electric-vehicle-adoption/. [Accessed: April 15, 2021].

[3] Tesla Models [online]. Available: https://www.tesla.com/model. [Accessed: May 1, 2021].

[4] Y. Wang, W. Ding, L. Huang, Z. Wei, H. Liu and J. A. Stankovic, "Toward Urban Electric Taxi Systems in Smart Cities: The Battery Swapping Challenge," in *IEEE Transactions on Vehicular Technology*, vol. 67, no. 3, pp. 1946-1960, March 2018, doi: 10.1109/TVT.2017.2774447.

[5] Q. Dai, T. Cai, S. Duan and F. Zhao, "Stochastic Modeling and Forecasting of Load Demand for Electric Bus Battery-Swap Station," in *IEEE Transactions on Power Delivery*, vol. 29, no. 4, pp. 1909-1917, Aug. 2014, doi: 10.1109/TPWRD.2014.2308990.

[6] Ahmad, F., Saad Alam, M., Saad Alsaidan, I. and Shariff, S.M, "Battery swapping station for electric vehicles: opportunities and challenges," *IET Smart Grid*, Vol. 3 no. 3, pp. 280-286 6, 2020, doi:10.1049/iet-stg.2019.0059.

[7] Y. Wang, K. Lai, F. Chen, Z. Li, and C. Hu, “Shadow price based co-ordination methods of microgrids and battery swapping stations,” *Appl. Energy*, vol. 253, pp. 1–16, Nov. 2019.

[8] H. Wu, G. K. H. Pang, K. L. Choy and H. Y. Lam, "An Optimization Model for Electric Vehicle Battery Charging at a Battery Swapping Station," in *IEEE Transactions on Vehicular Technology*, vol. 67, no. 2, pp. 881-895, Feb. 2018, doi: 10.1109/TVT.2017.2758404.

[9] Y. Zheng, Z. Y. Dong, Y. Xu, K. Meng, J. H. Zhao and J. Qiu, "Electric Vehicle Battery Charging/Swap Stations in Distribution Systems: Comparison Study and Optimal Planning," in *IEEE Transactions on Power Systems*, vol. 29, no. 1, pp. 221-229, Jan. 2014, doi: 10.1109/TPWRS.2013.2278852

[10] M. R. Sarker, H. Pandžić and M. A. Ortega-Vazquez, "Optimal Operation and Services Scheduling for an Electric Vehicle Battery Swapping Station," in *IEEE Transactions on Power Systems*, vol. 30, no. 2, pp. 901-910, March 2015, doi: 10.1109/TPWRS.2014.2331560.

[11] X. Liu, T. Zhao, S. Yao, C. B. Soh and P. Wang, "Distributed Operation Management of Battery Swapping-Charging Systems," in *IEEE Transactions on Smart Grid*, vol. 10, no. 5, pp. 5320-5333, Sept. 2019, doi: 10.1109/TSG.2018.2880449.

[12] S. Esmaeili, A. Anvari-Moghaddam and S. Jadid, "Optimal Operation Scheduling of a Microgrid Incorporating Battery Swapping Stations," in *IEEE Transactions on Power Systems*, vol. 34, no. 6, pp. 5063-5072, Nov. 2019, doi: 10.1109/TPWRS.2019.2923027.

[13] H. Liu, Y. Zhang, S. Ge, C. Gu and F. Li, "Day-Ahead Scheduling for an Electric Vehicle PV-Based Battery Swapping Station Considering the Dual Uncertainties," in *IEEE Access*, vol. 7, pp. 115625-115636, 2019, doi: 10.1109/ACCESS.2019.2935774.

[14] N. Liu, Q. Chen, X. Lu, J. Liu and J. Zhang, "A Charging Strategy for PV-Based Battery Switch Stations Considering Service Availability and Self-Consumption of PV Energy," in *IEEE Transactions on Industrial Electronics*, vol. 62, no. 8, pp. 4878-4889, Aug. 2015, doi: 10.1109/TIE.2015.2404316.

[15] M. Ban, M. Shahidehpour, J. Yu and Z. Li, "A Cyber-Physical Energy Management System for Optimal Sizing and Operation of Networked Nanogrids With Battery Swapping Stations," in *IEEE Transactions on Sustainable Energy*, vol. 10, no. 1, pp. 491-502, Jan. 2019, doi: 10.1109/TSTE.2017.2788056.

[16] X. Tan, G. Qu, B. Sun, N. Li and D. H. K. Tsang, "Optimal Scheduling of Battery Charging Station Serving Electric Vehicles Based on Battery Swapping," in *IEEE Transactions on Smart Grid*, vol. 10, no. 2, pp. 1372-1384, March 2019, doi: 10.1109/TSG.2017.2764484.

[17] S. Stüdli, W. Griggs, E. Crisostomi and R. Shorten, "On Optimality Criteria for Reverse Charging of Electric Vehicles," in IEEE *Transactions on Intelligent Transportation Systems*, vol. 15, no. 1, pp. 451-456, Feb. 2014, doi: 10.1109/TITS.2013.2271953.

[18] X. Zhang, Y. Cao, L. Peng, N. Ahmad and L. Xu, "Towards Efficient Battery Swapping Service Operation Under Battery Heterogeneity," in *IEEE Transactions on Vehicular Technology*, vol. 69, no. 6, pp. 6107-6118, June 2020, doi: 10.1109/TVT.2020.2989195.

[19] M. H. Amini, O. Karabasoglu, M. D. Ilić, K. G. Boroojeni and S. S. Iyengar, "ARIMA-based demand forecasting method considering probabilistic model of electric vehicles' parking lots," 2015 *IEEE Power & Energy Society General Meeting, Denver,* CO, 2015, pp. 1-5, doi: 10.1109/PESGM.2015.7286050.

[20] R. Khodabakhsh and S. Sirouspour, "Optimal Control of Energy Storage in a Microgrid by Minimizing Conditional Value-at-Risk," in *IEEE Transactions on Sustainable Energy,* vol. 7, no. 3, pp. 1264-1273, July 2016, doi: 10.1109/TSTE.2016.2543024.

[21] J. Zhang, X. Mu, J. Fang and Y. Yang, "Time Series Imputation via Integration of Revealed Information Based on the Residual Shortcut Connection," in *IEEE Access*, vol. 7, pp. 102397-102405, 2019, doi: 10.1109/ACCESS.2019.2928641.

[22] L. Sehovac and K. Grolinger, "Deep Learning for Load Forecasting: Sequence to Sequence Recurrent Neural Networks With Attention," in *IEEE Access*, vol. 8, pp. 36411-36426, 2020, doi: 10.1109/ACCESS.2020.2975738.

[23] Q. Kang, J. Wang, M. Zhou and A. C. Ammari, "Centralized Charging Strategy and Scheduling Algorithm for Electric Vehicles Under a Battery Swapping Scenario," in *IEEE Transactions on Intelligent Transportation Systems*, vol. 17, no. 3, pp. 659-669, March 2016, doi: 10.1109/TITS.2015.2487323.

[24] R. Khodabakhsh and S. Sirouspour, "Optimal Control of Energy Storage in a Microgrid by Minimizing Conditional Value-at-Risk," in *IEEE Transactions on Sustainable Energy*, vol. 7, no. 3, pp. 1264-1273, July 2016, doi: 10.1109/TSTE.2016.2543024.

[25] Peters, Diane L., Mechtenberg, Abigail R., Whitefoot, John, and Papalambros, Panos Y. "Model Predictive Control of a Microgrid With Plug-In Vehicles: Error Modeling and the Role of Prediction Horizon," *ASME 2011 Dynamic Systems and Control Conference and Bath/ASME Symposium on Fluid Power and Motion Control*, Volume 1. Arlington, Virginia, USA. October 31–November 2, 2011. pp. 787-794. ASME.

[26] A. O'Connell, A. Keane and D. Flynn, "Rolling multi-period optimization to control electric vehicle charging in distribution networks," *2014 IEEE PES General Meeting | Conference & Exposition, National Harbor*, MD, 2014, pp. 1-1, doi: 10.1109/PESGM.2014.6938830.

[27] M. Zeng, Y. Pan, D. Zhang, Z. Lu and Y. Li, "Data-Driven Location Selection for Battery Swapping Stations," in *IEEE Access*, vol. 7, pp. 133760-133771, 2019, doi: 10.1109/ACCESS.2019.2941901.

[28] P. You *et al*., "Scheduling of EV Battery Swapping—Part I: Centralized Solution," in *IEEE Transactions on Control of Network Systems*, vol. 5, no. 4, pp. 1887-1897, Dec. 2018, doi: 10.1109/TCNS.2017.2773025.

[29] P. You *et al*., "Scheduling of EV Battery Swapping–Part II: Distributed Solutions," in *IEEE Transactions on Control of Network Systems*, vol. 5, no. 4, pp. 1920-1930, Dec. 2018, doi: 10.1109/TCNS.2017.2774012.

[30] P. Fan, B. Sainbayar and S. Ren, "Operation Analysis of Fast Charging Stations With Energy Demand Control of Electric Vehicles," in *IEEE Transactions on Smart Grid*, vol. 6, no. 4, pp. 1819-1826, July 2015, doi: 10.1109/TSG.2015.2397439.

[31] Q. Yang, S. Sun, S. Deng, Q. Zhao and M. Zhou, "Optimal Sizing of PEV Fast Charging Stations With Markovian Demand Characterization," in *IEEE Transactions on Smart Grid*, vol. 10, no. 4, pp. 4457-4466, July 2019, doi: 10.1109/TSG.2018.2860783.

[32] S. Sun, Q. Yang and W. Yan, "Hierarchical optimal planning approach for plug-in electric vehicle fast charging stations based on temporal-SoC charging demand characterisation," in *IET Generation, Transmission & Distribution*, vol. 12, no. 20, pp. 4388-4395, 13 11 2018, doi: 10.1049/iet-gtd.2017.1894.

[33] Hochreiter, S.; Schmidhuber, J. Long short-term memory. Neural Comput. 1997, 9, 1735–1780.

[34] GAMS –A User's Guide [Online] Available: https://www.gams.com/latest/docs/gams.pdf. [Accessed: May 1, 2021].

[35] Time series forecasting using deep learning [online]. Available: https://www.mathworks.com/help/deeplearning/ug/time-series-forecasting-using-deep-learning.html. [Accessed: May 1, 2021].

[36] D. Singh, R. K. Misra and D. Singh, "Effect of Load Models in Distributed Generation Planning," in *IEEE Transactions on Power Systems*, vol. 22, no. 4, pp. 2204-2212, Nov. 2007, doi: 10.1109/TPWRS.2007.907582

Vita

Ahmed Ayman Ahmed Shalaby was born in 1995, in Cairo, Egypt. He received his primary and secondary education in Cairo, Egypt. He received his B.Sc. degree in Electrical Engineering from the Faculty of Engineering Ain Shams University in 2018.

In January 2020 he joined the Electrical Engineering master's program at the American University of Sharjah as a graduate research assistant. During his master's study, he co-authored 4 papers that were presented in international conferences and journals. His research interests are mainly planning and operational challenges in smart grids, Distributed energy resources, Energy storage systems, and optimization in power systems and smart grids.